MASTER THESIS

Linn Hjelmeland Svendheim
BI309F MSc in Marine Ecology

Seasonal progression of the zooplankton community in a high Arctic fjord and the main physical and biological drivers

Date: 22.05.2017 Total number of pages: 60

NORD University

www.nord.no

Abstract
This study follows the seasonal progression of the zooplankton community in Van Mijenfjorden, an Arctic sea ice covered sill fjord on the west coast of Svalbard. Van Mijenfjorden is influenced by locally produced Local water masses and Winter Cooled water masses, and by Atlantic Water (AW) from the West Spitsbergen Current. The fjord show great variability in hydrography due to tidal exchange and wind forcing. Several influxes of AW were recorded during winter, but this did not seem to influence the zooplankton community. Zooplankton abundances were low in spring, but started to increase from May onwards with maximum abundances recorded in August at the end of the study. Two peaks in meroplankton were found, Cirripedia nauplii in June, and Bivalvia veligers in July, which was the main reason for the high zooplankton abundances recorded in this study. The dominant copepod species in this study was *Oithona similis*, *Calanus* spp, and *Pseudocalanus* spp.. These copepods had different timing in reproduction. *Calanus glacialis* started to reproduce in April with peak egg production rates in May. *Calanus finmarchicus* reproduced in June, *Pseudocalanus* spp. in July and *O. similis* in August. Both *C. glacialis* and *C. finmarchicus* were present in Van Mijenfjorden in September 2015, and in March 2016 suggesting that they both are capable of overwintering in the fjord. However, it is not likely that they have sustainable populations in this fjord, since both species prefer deeper overwintering depths and previous data show very poor abundances of *Calanus* spp. in Van Mijenfjorden. The zooplankton community in Van Mijenfjorden was influenced mainly by local processes in 2016.

Acknowledgements
This master thesis was written at Nord University, Faculty of Biosciences and Aquaculture, and was part of the FAABulous project (Future Arctic Algae Blooms - and their role in the context of climate change), funded by the Research Council of Norway, project nr. 243702. The fieldwork was conducted from the University Center in Svalbard (UNIS).

Thank you to my supervisors, Vigdis Tverberg and Janne E. Søreide for supporting me and giving me feedback throughout this process, and for answering all the million questions I have had with a positive attitude and optimism. To be able to work on this project has given me experience in writing, fieldwork and labwork, and so many new and exciting experiences.

I must thank Maja Hatlebakk (PhD Nord University, UNIS), without whom I would be lost at UNIS. Thank you for all your help in the field and in the lab, and for just being the person I could ask about anything and everything. And I thank Kanchana Bandara (PhD Nord University) for all your much-needed help with R.

Thank you to Ane and Magda for great help in field onboard Viking Explorer together with Maja. Thank you to my classmate Sofie, without whom the lab work and writing process would have been much harder. Also, thank you to my family for your support, and to my husband for letting me disappear to Svalbard for nine months.

Content

List of figures

List of tables

Abbreviations

AF	Adult female
AM	Adult male
ArW	Arctic water mass
AW	Atlantic water mass
C I-CV	Copepodite stage 1-5
Chl-*a*	Chlorophyll-*a*
CTD	Conductivity Temperature and Density profiler
EPR	Egg production rate
ESC	East Spitsbergen Current
LW	Local water mass
N I-VI	Nauplii stage 1-6
PL	Prosome length
RDA	Redundancy analyzes
TAW	Transformed Atlantic water mass
TL	Total lipids
TS plot	Temperature and salinity plot
vMF 1-9	Sampling stations in Van Mijenfjorden
WSC	West Spitsbergen Current
WCW	Winter cooled water mass

1.0 Introduction

High latitude marine ecosystems experience strong seasonality in abiotic factors such as light, temperature and wind, which in turn leads to seasonal changes in the biological production (Varpe, 2012). In Svalbard, the sun is below the horizon for almost 4 months in winter, and in regions with sea ice this period of darkness will be extended further, sometimes for 3-4 months more. Light measurements from sea observatories in Svalbard fjords show that sufficient light to initiate the spring phytoplankton bloom may differ with up to 2 months in ice free versus seasonal ice covered fjords (Berge et al., 2014). How secondary producers cope with this strong seasonality is less known since studies following the seasonal progression in one region/system are few. In Svalbard, the seasonal development of the zooplankton community has been studied in Rijpfjorden (Søreide et al., 2010, Leu et al., 2011, Weydmann et al., 2013) and to some extent in Hornsund, Kongsfjorden and Isfjorden/Adventfjorden (Kwasniewski et al., 2003, Walkusz et al., 2009, Stubner et al., 2016).

In Arctic systems, the zooplankton community structure changes with the seasons, from low numbers and low biomass during winter and spring to high abundance and biomass in autumn (Walkusz et al., 2009). In seasonally ice covered fjords an ice algal bloom is commonly starting in spring before the ice melts, presenting an important early food source before it is followed by a pelagic phytoplankton bloom when the ice breaks up (Leu et al., 2011). The timing of the ice algal bloom depends on the solar angle, ice thickness and snow cover (Mundy et al., 2005). Deeper snow and thicker ice delays the start of the bloom, while a thin snow cover and thin ice will shorten the ice algal bloom as the ice melts faster (Mundy et al., 2005). In Rijpfjorden in North-East Svalbard, the phytoplankton bloom is delayed by 2-3 months, and the zooplankton community succession by 1-2 months compared to the open year-round Kongsfjorden in Western Svalbard (Weydmann et al., 2013).

The most abundant zooplankton species in Svalbard waters are the small copepods *Oithona similis* (Claus, 1866), *Microcalanus* spp and *Pseudocalanus* spp., while the relatively large copepods of the genus *Calanus spp.*: *Calanus finmarchicus* (Gunnerus, 1770), *Calanus glacialis* (Jaschnov, 1955) and *Calanus hyperboreus* (Krøyer 1838) comprises most of the zooplankton biomass (Willis et al., 2006, Blachowiak-Samolyk et al., 2008, Walkusz et al., 2009, Hirche and Kosobokova, 2011, Weydmann et al., 2013, Gluchowska et al., 2016).

Calanoid copepods are key species in the Arctic pelagic food web due to their ability to convert the low-energy carbohydrates from their algal diet into high-energy wax ester lipids (Falk-Petersen et al., 2009). This makes them very valuable food items for higher trophic levels like fish and sea birds (Conover, 1988, Falk-Petersen et al., 2002, Falk-Petersen et al., 2007, Daase et al., 2013). The three species in the genus *Calanus* co-excist in the dynamic Svalbard region where warmer Atlantic waters meets colder Arctic waters. *C. glacialis* is considered an Arctic shelf species, and is consistently found in the waters north of the polar front (Tande, 1991, Falk-Petersen et al., 2009). *C. hyperboreus* is larger in size and lipid reserves, and has its main distribution area in the Greenland Sea, but expatriates south to the Norwegian Sea (Conover, 1988, Falk-Petersen et al., 2009). *C. finmarchicus* is transported north with Atlantic water masses in the West Spitsbergen Current (WSC), and co-exist with *C. glacialis* in areas where Arctic and Atlantic water masses meet and mixes (Conover, 1988, Tande, 1991, Hirche and Kosobokova, 2007).

All three species develop through six nauplii stages (NI-NVI) and five copepodite stages (CI-CV) before molting into adult females (AF) or adult males (AM) (Falk-Petersen et al., 2009, Søreide et al., 2010). In areas with a long-lasting ice cover, like Rijpfjorden, *C. glacialis* utilize lipid stores and the ice algal bloom (Runge and Ingram, 1988, Daase et al., 2013) to fuel reproduction under the ice. The nauplii will then reach the first feeding stage (NIII) at the onset of the phytoplankton bloom (Leu et al., 2011, Daase et al., 2013). *C. glacialis* spend the winter in diapause at depth (Conover, 1988, Kosobokova, 1999), and the main overwintering stages are CIV and CV, but they may also overwinter as CIII (Madsen et al., 2001, Falk-Petersen et al., 2009). Those able to reach CV will complete their life cycle in 1 year, those that reach CIV will spend 2 years to complete the life cycle (Falk-Petersen et al., 2009, Søreide et al., 2010, Daase et al., 2013).

C. finmarchicus seems to time its spawning to the phytoplankton bloom in April-May in the Barents Sea. They are smaller, and less lipid rich than *C. glacialis* (Hirche and Kosobokova, 2007, Falk-Petersen et al., 2009), and reach the overwintering stages CIV and CV by July, and usually has a 1 year life cycle around the polar front and in the Barents Sea (Tande, 1991, Madsen et al., 2001, Falk-Petersen et al., 2009). *C. finmarchicus* may not be able to successfully complete their life cycle in Arctic waters due to low temperature, and short growing season (Hirche and Kosobokova, 2007, Ji et al., 2012). This situation might be about to change due to the rapid climatic changes in the Arctic, causing warming of the ocean, and thinning of the sea ice (Johannessen et al., 2004, Hirche and Kosobokova, 2007).

Frost (1989) found that two of the seven *Pseudocalanus* species; *Pseudocalanus acuspes* (Giesbrecht, 1881) and *Pseudocalanus minutus* (Krøyer, 1845) were present in Svalbard waters. They are considered Arctic species, and have more lipids compared to more temperate species (Bailey et al., 2016). It has later also been discovered a third species present in Svalbard, *Pseudocalanus moultoni* (Frost, 1989, Aarbakke et al., 2011). *Pseudocalanus* spp. are opportunistic feeders, with a wide diet (Cleary et al., 2016), and are active and breed throughout the year, with the main breeding season from April to May, and low numbers in winter (Halsband and Hirche, 2001).

The small cyclopoid copepod *O. similis*, is an opportunistic species, with distribution in all the world's oceans (Ward and Hirst, 2007). It is often reported to be the dominant species in terms of abundance (Blachowiak-Samolyk et al., 2007, Hirche and Kosobokova, 2011, Gluchowska et al., 2016), which might be due to the species ability to survive and reproduce at a wide range of temperatures (Ward and Hirst, 2007). In Kongsfjorden, *O. similis* has shown a seasonal cycle in abundance, with peak abundance in November, and lowest abundance in June (Lischka and Hagen, 2005). Due to their omnivorous diet, they are not dependent on the spring bloom and reproduce all year, with peaks in May-June and August-September (Lischka and Hagen, 2005, Ward and Hirst, 2007).

Meroplankton spend part of their life in the pelagic realm before they settle, often as benthic invertebrates, and are therefore often omitted from plankton studies (Stübner et al. 2016). A study in Isfjorden/Adventfjorden, showed that meroplankton contributed little to the total zooplankton biomass outside the reproductive season, but overall throughout the year they comprised 76% of the total zooplankton abundance (Stübner et al., 2016). This was largely due to a peak of Cirripedia larvae in late April - beginning of May, and a peak of Bivalvia veliger larvae from the end of May to the beginning of July (Stübner et al., 2016).

Due to its planktonic state, the composition and distribution of the zooplankton community is influenced by the origin of water masses and hydrophysical processes (Saloranta and Svendsen, 2001, Basedow et al., 2004, Willis et al., 2006, Willis et al., 2008). The fjords situated on the West Spitsbergen shelf are influenced by two currents (Fig. 1), the before mentioned WSC bringing warm, saline Atlantic water (AW > 34.9PSU, >3ºC)

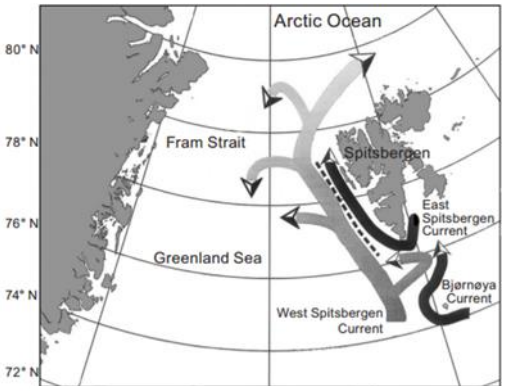

Figure 1 Map showing the currents that converge and mix in the frontal zone (dotted line) on the west side of Spitsbergen (Saloranta and Svendsen, 2001)

northward, and the East Spitsbergen Current (ESC) transporting colder, less saline Arctic water (ArW 34.3 – 34.8PSU, -1.5 – 1.0ºC) northward (Svendsen et al., 2002, Cottier et al., 2005). The Arctic Front on the shelf, is where these two water masses converge, mixing into Transformed Atlantic Water (TAW) (Saloranta and Svendsen, 2001, Cottier et al., 2005).

Several studies have shown that advection of water masses into the fjords play a significant role in shaping the zooplankton community, as well as influencing bloom dynamics and nutrient supply (Basedow et al., 2004, Wills et al., 2006, Willis et al., 2008, Walkusz et al., 2009). In areas where advection of water masses is high, local production can be exceeded by immigrating populations by a factor of four (Basedow et al., 2004). In Kongsfjorden, Basedow et al. (2004) proposes that *C. glacialis* have locally producing populations in the inner part of the fjord, where the water is colder, and with weaker currents, while *C. finmarchicus* that spawn on the shelf might be advected into the fjord with the shelf water (TAW), and thereby make the fjord able to support larger populations of higher trophic levels. Whether this process also happens in the same scale in more closed fjords, like Van Mijenfjorden, is not known.

1.1 Objectives

In this study, I followed the seasonal progression of the zooplankton community composition in Van Mijenfjorden, a seasonally ice covered fjord on west-Spitsbergen. The main aim was to study the physical and biological drivers shaping the zooplankton community in this so far poorly studied fjord.

The following research questions were addressed:

1) Is the hydrography the main driver of shaping the zooplankton community in Van Mijenfjorden?
2) Which species comprise the largest part of the zooplankton community in Van Mijenfjorden?
3) Do *Calanus glacialis* and *Calanus finmarchicus* have sustainable populations in this shallow sill fjord?

2.0 Materials and Methods

2.1 Study site

Van Mijenfjorden is located on the west coast of Spitsbergen. The fjord is 60 km long, with an average width of 10 km. The fjord consists of two basins, one deep basin with a maximum depth of 115 m deep, and one shallower, inner basin, with a maximum depth of 74 m. The two basins are separated by a 45 m sill (Fer and Widell, 2007, Skarðhamar and Svendsen,

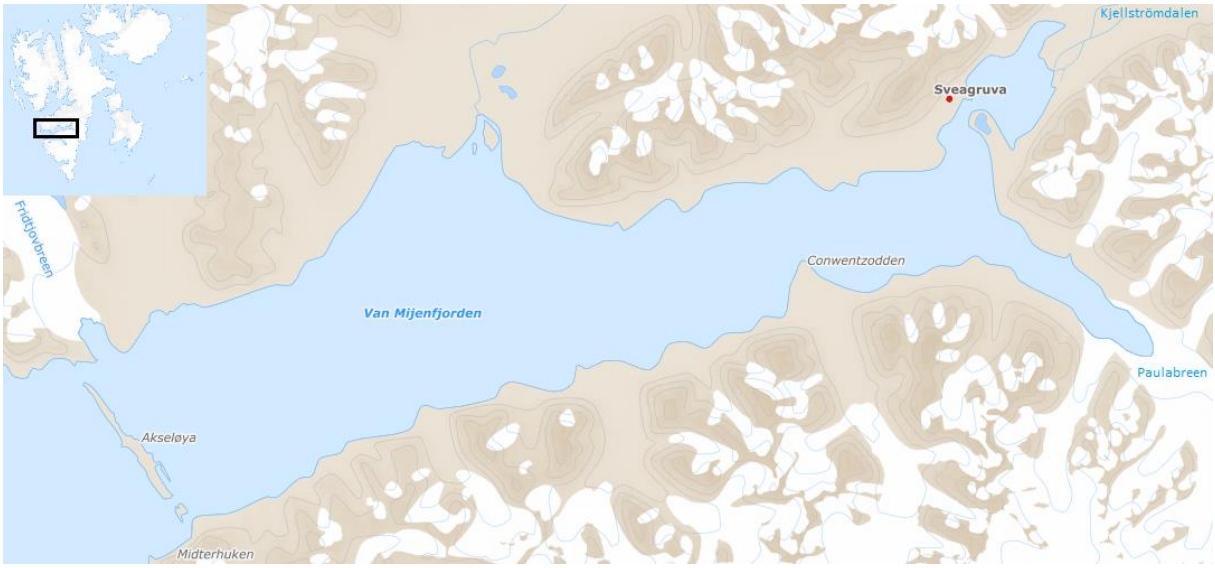

Figure 2 Van Mijenfjorden, situated on the west coast of Spitsbergen, with the two glaciers, Fridtjovbreen and Paulabreen, that calves into the fjord. (Norkart AS, 2017).

2010). The fjord is broad in relation to the baroclinic Rossby radius, making rotational dynamics important, especially in the outer basin, which is broader than the inner basin (Skarðhamar and Svendsen, 2010). Currents will then tend to follow the shore on its right side. The fjord is almost closed off at the mouth by Akselsøya (Fig. 2). Water exchange can only take place through the two narrow sounds on either side of the island. The main water exchange takes place through Akselsundet in the north, which is 1 km wide, with a shallow sill of 34 m. The sound on the southern side, Mariasundet, is very shallow (2 -12 m) and is divided by an islet, creating only a 600m wide passage on one side, and 500m on the other (Fer and Widell, 2007, Skarðhamar and Svendsen, 2010).

Several rivers discharge into Van Mijenfjorden, adding freshwater particularly during the melting season. This process forms a Surface Water (SW) layer with low salinity (Cottier et al., 2010). In addition, two glaciers calve into the fjord, Paulabreen and Fridtjovbreen (Fig. 2). The meltwater causes the fjord to be stratified during summer and autumn (Støylen and Fer, 2014). When the fjord is ice free, wind effects are pronounced in Van Mijenfjorden due to its semi-enclosed nature (Skarðhamar and Svendsen, 2010). The wind field usually has an easterly down fjord component, especially during winter (Hanssen-Bauer et al., 1990). The

circulation in the fjord during summer is based on the combined result of wind effects, Coriolis force and the estuarine circulation (Skarðhamar and Svendsen, 2010), creating a fresh current in the surface that is directed out of the fjord on the north side (Skarðhamar and Svendsen, 2010) This current is enhanced during easterly wind directions due to the geostrophic current set up by the pressure gradient caused by Ekman transport (Cottier et al., 2010, Skarðhamar and Svendsen, 2010).

Tidal currents are strong due to the narrow entrance to the fjord, and keeps the two sounds ice free all year (Skarðhamar and Svendsen, 2010). The tidal currents that are forced over obstacles like the shallow Akselsundet, can give rise to internal Kelvin waves on the thermocline. In Van Mijenfjorden such internal waves propagate cyclonically around the fjord, creating a mean current inward on the southside, and out the fjord on the north side. When the waves break, they increase the vertical mixing (Mann and Lazier, 2006, Skarðhamar and Svendsen, 2010, Støylen and Fer, 2014). The water circulation in Van Mijenfjorden is subjected to high frequency variations due to the changing wind pattern and tidal mixing (Skarðhamar and Svendsen, 2010 Støylen and Fer, 2014).

During ice cover formation in winter, brine is released to the water column, increasing the salinity and density of the surface water. The water column becomes unstable, and haline driven convection mixes the water column (Haarpaintner et al., 2001, Cottier et al., 2010). Winter Cooled Water (WCW) is produced by this process, with very low temperatures and high salinity. The water mass is very dense, and can remain at the bottom of the fjord the entire year (Cottier et al., 2010). Also, cold and less saline Local Water (LW) is produced by convective mixing due to cooling of the surface in autumn (Cottier et al., 2010).

Van Mijenfjorden is considered a good study site for process studies due to its closed nature, restricting the water exchange (Fer and Widell, 2007, Skarðhamar and Svendsen, 2010, Støylen and Fer, 2014).

2.2 Sampling stations

The FAABulous project has several fixed sampling stations in the fjord, as well as one on the outside. For this study, it was decided to sample in the innermost basin (vMF 1), the outer basin (vMF 5), and just outside the fjord (vMF 9) for an outside reference (Fig. 3).

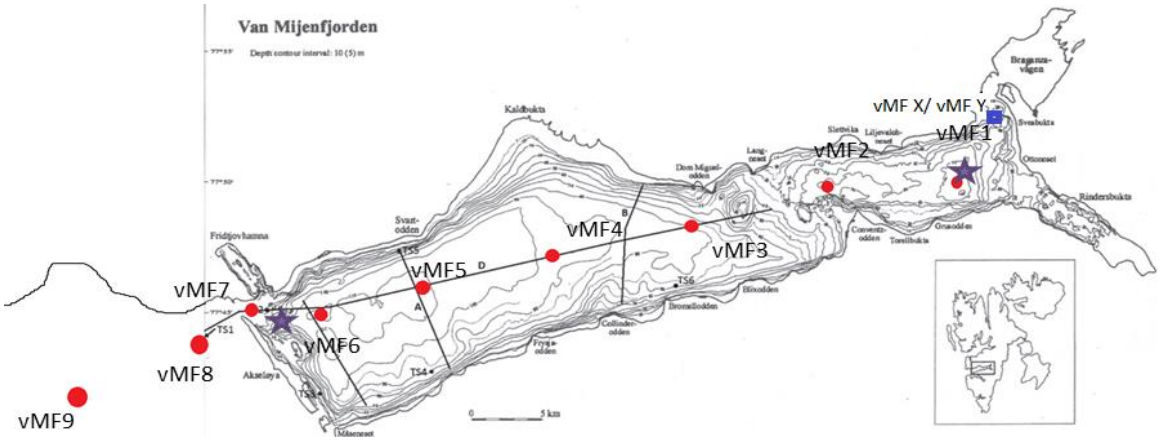

Figure 3 Overview of sampling stations in Van Mijenfjorden (FAABolous project). The main sampling stations were vMF1, vMF5 and vMF9. The star in the inner part of the fjord represent the Miracle mooring, and the star I the outer part represent the mooring that was lost. The sampling sites for March (vMF X) and April (vMF Y) from the sea ice are shown with a blue square.

In March and April, the sampling site was reached by snow mobiles using the sea ice as sampling platform. Drift ice near the fjord prevented boats to enter the fjord. The ice conditions in 2016 were particularly poor, and sampling from a sea ice platform was only possible to conduct closer to shore (vMF X and vMF Y) (Fig.3, Table 1) where the ice was safe to travel on.

Table 1 Overview of station names, position, and bottom depth in this study.

Station	Coordinate	Depth (m)
vMF X	77.8817N 16.7403E	20
vMF Y	77.8697N 16.7478E	33
Miracle mooring	77.8292N 16.6125E	75.5
vMF 1	77.8314N 16.6195E	78
vMF 3	77.7940N 15.8085E	88
vMF 4	77.7933N 15.4832E	-
vMF 5	77.7669N 15.0444E	116
vMF 9	77.6899N 14.0913E	140

In May, all the planned regular sampling sites were sampled by boat, except the innermost station vMF1 where sea ice was still present. Station vMF 3 was therefore the innermost

station sampled in April/May (Fig. 3 and Fig. 4). In addition, vMF 4 was chosen over vMF 5 in May due to the particularly high fluorescence readings here (Fig 3, Table 1). In June, July, and August the sampling schedule went as planned, and the stations vMF1, vMF5 and vMF9 were sampled.

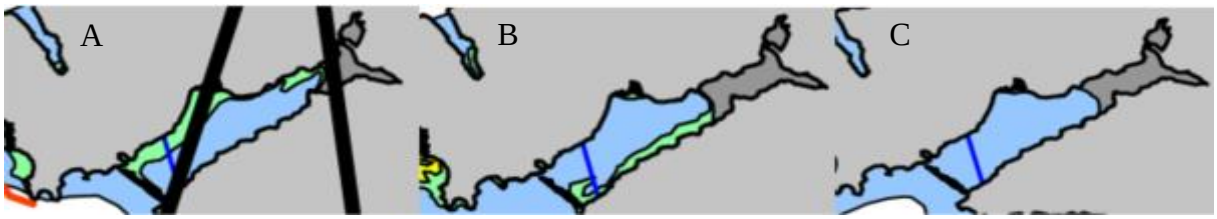

Figure 4 Overview of the ice extent in Van Mijenfjorden on March 9th, April 14th and April 29th 2016. Grey areas are fast ice, and green areas represent very open drift ice (Norwegian Ice Service – MET Norway, Norwegian Meteorological Institute, 2017).

2.3 Sampling

2.3.1 Hydrographic sampling

CTD profiles were taken at vMF X and vMF Y in March and April 2016. A CTD transect was performed on every sampling trip by boat. The fluorometer on the CTD was not calibrated, but as the same CTD was used for all except two transects, the fluorescence data can be compared among months as a proxy of algal food being abundant or not. The CTD used was a SAIV SD204 on all transects, except from the sampling on the 15th of May and in August. On these two trips the research vessel Helmer Hanssen was used, and a Seabird 911 plus mounted on a rosette with 12 Niskin water sampling bottles. Water samples (5m – 10 m – 15 m – 25 m – 50 m -bottom) were collected by other participants in the FAABolous project on the same sampling stations as the zooplankton samples (Table 2).

In September 2015 two moorings were deployed. One mooring was deployed close to vMF 1 (Miracle mooring), in the inner basin of the fjord, and the other near the fjord mouth, on the inside of Akselsundet (Fig. 3). Retrieval of the inner basin mooring was successful in August 2016, but the outer mooring was lost.

The mooring length of the innermost mooring was 67,5 m, and the distance from its subsurface buoy to the surface was 8 m. A Seabird 16+ recorder (SBE 16+) was mounted at 12,5 m measuring conductivity, temperature, pressure, fluorescence, and PAR (photosynthetically active radiation). A McLane RAS 500 water sampler was mounted at ~14 m, with additional sampling gear for pH and UV measurements. An upward looking Teledyne RDI 300kHz ADCP was mounted at ~64 m, measuring current profiles. At ~6 8m a

Seabird MicroCAT CTD (SBE37sm) was placed, measuring temperature and salinity. In addition, six Seabird temperature loggers (SBE56) were placed throughout the mooring - string.

2.3.2 Zooplankton community

The zooplankton community was sampled by a closing WP2 net (UNESCO, 1968) with a net opening of 0.25 m² and mesh size of 64 µm. Three replicates were sampled per station to capture the variability and patchiness in the zooplankton distribution. When sampling locations were deeper than 50 m, the water column was divided into two sampling depth strata: bottom – 20 m, and 20 m – surface, each with three replicates, resulting in six samples per station (Table 2). To avoid sediments in the net, the net was lowered to maximum ~10 m above bottom.

Reference samples from autumn 2015 were sampled from stations vMF 1 and vMF 5 (Fig 3, Table 2). Here a WP2 net with a mesh size of 200 µm was used and five replicates of the zooplankton community composition were sampled from bottom to surface. However, only three samples from each station were analyzed in this study. Because of clogging of the 64 µm net due to algal blooms during the June sampling campaign, the community samples were collected with a net with coarser mesh size (200 µm) this month (Table 2).

The zooplankton samples were preserved in 4% formaldehyde-sea water solution buffered with hexamine within 1 hour of collection. Any jellies were taken out prior to fixation.

2.3.3 Zooplankton biomass

In addition to zooplankton community samples, net samples for zooplankton biomass were collected (Table 2). These samples were collected from bottom to surface with the same WP2 net as for the community samples (Table 2). Because of time constraints, three replicates were not always possible to collect for all stations (Table 2). The samples were frozen just after sampling without any fixatives added.

Table 2 Overview of date, location, and sampled parameters. For zooplankton samples, nets were sampled from 0 – 20 m and 20 m - bottom in triplicates, resulting in six samples per station. Biomass samples were from bottom to surface. In addition to the samples shown, a CTD was taken at each station. For station information see Figure 2, Table 1. *zooplankton nets sampled bottom to surface.

Date	Station	Zooplankton net	Biomass	Egg incubation
23.– 24.09.15	vMF 1	5 x 200µm*		
	vMF 5	5 x 200µm*		
09.03.16	vMF X	3 x 64µm*		
14.04.16	vMF Y	3 x 64µm*		x
30.04. – 01.05.16	vMF 3	6 x 64µm	1 x 64µm	
	vMF 4	6 x 64µm	3 x 64µm	
	vMF 5			x
	vMF 9	6 x 64µm	2 x 64µm	
15.05.16	vMF 1	3 x 200µm*		
03.– 04.06. 16	vMF 1	2 x 64µm, 4 x 200µm	1 x 200µm	x
	vMF 5	2 x 64µm, 4 x 200µm	1 x 200µm	x
	vMF 9	2 x 64µm, 4 x 200µm	1 x 200µm lost	
02.– 04.07.16	vMF 1	6 x 64µm	3 x 64µm	x
	vMF 5	6 x 64µm	2 x 64µm	x
	vMF 9	6 x 64µm	2 x 64µm	
19.– 20.08.16	vMF 1	6 x 64µm	1 x 64µm	x
	vMF 5	6 x 64µm	1 x 64µm	x
	vMF 9	1 x 64µm*		

2.3.4 Egg incubations

Live animals for the incubation of *Calanus* spp. AF were collected in April from the ice station, in the beginning of May from station vMF 5, and for the remaining sampling trips from both vMF1 and vMF 5 (Fig. 3, Table 2). The aim was to incubate 30 females of both *C. glacialis* and *C. finmarchicus*. The females were determined to species based on red pigmentation (Nielsen et al., 2014) as prosome length may overlap considerably between these two species (Gabrielsen et al., 2012). In April, very few females were found, and in May, only females of *C. glacialis*. From June onwards, a mix of the two species were incubated because it was difficult to find 30 of each. Therefore, the numbers varied from month to month (Table 6).

Live AF for egg incubations were collected by a WP2 net with a diameter of 0.25 m², and a mesh size of 64 µm in April, and a mesh size of 200 µm in May and June. In July and August, a WP3 net was used, with an opening of 1 m^3 and a mesh size of 1000 µm. Only the upper 20 – 50 m were sampled.

The AF were sorted under the stereomicroscope, in dishes placed on ice to avoid overheating of the animals. The incubation water was collected from the surface at the same site as the AF were collected. The water was filtered through a 50 – 64 µm sieve to remove larger organisms. For the incubation two cups placed within each other were used, with the inner cup having a false bottom, with a mesh size of 500 µm or 1000 µm to allow the eggs to fall through, without letting the AF through to predate on their own eggs (Fig. 5). One AF was placed in each cup. The incubation cups were placed in a cooler on deck with freezing elements. The temperature was noted before and after the experiment, except in June and July when Hobo-loggers were used to record the temperature every 5 minutes. The incubation lasted for 24 hours. In some cases, it was impractical to end the experiment after exactly 24 hours. When this occurred, the result was standardized to represent a 24-hour incubation period. The experiments were ended by separating the AF from the cups containing the eggs.

Figure 5 Cups with mesh bottom for incubation of *Calanus* spp. AF. The AF is kept in the top cup, while the eggs will sink to the bottom.

2.4 Sample analyses

2.4.1 Hydrographic analysis

The CTD profile data were analyzed using Ocean Data View 4.7.7. (Schlitzer, 2016) for each monthly transect for the main water parameters salinity, temperature, and fluorescence. Mooring data from the SBE 16+ at 12 m, and the SBE37sm at 68 m were also analyzed using Ocean Data View 4.7.7 (Schlitzer, 2016), as well as Rstudio 1.0.136 (R Core Team, 2016) and MATLAB (Matlab R2016a, 2016), creating time series of mooring data and TS plots of the same time series, overlaid with CTD profiles from the innermost station, vMF1.

In addition to measuring fluorescence, water samples from selected depths were taken for determination of the Chlorophyll a (Chl-*a*) biomass with a 10 L Niskin bottle. For Chl-*a* triplicates of 200-400 mL were filtered through glass microfiber filters (GF/F, 0.7µm,

Whatman, England). Filters were either stored frozen (-80°C) or Chl-*a* was extracted immediately in 10 mL methanol (~99%) for 20-24 h at 4°C in darkness (Holm-Hanssen and Riemann, 1978). Chl-*a* concentrations were measured with a calibrated fluorometer (10 AU-005-CE Fluorometer, Turner, USA; Chl a standard: Sigma S6144).

2.4.2 Zooplankton community analysis

The samples were diluted into a known volume (250 ml – 600 ml), from which subsamples of 2.5-5 ml were taken depending on the density of the sample by using an automatic pipette. Every organism in the subsample was counted and identified under the stereomicroscope, and additional subsamples were taken until the total number of individuals reached 300 or more. Jellies were identified to class Hydrozoa or phylum Ctenophora, and other zooplankton were identified to lowest possible taxonomic unit. *Pseudocalanus* spp. were analyzed to developmental stage. For *Calanus* spp. additional subsamples were counted to reach 100 individuals of *Calanus* spp. per sample. These where identified to copepodite developmental stage, and prosome length (PL) were measured to identify them to species (*C. glacialis, C. finmarchicus and C. hyperboreus*) according to Daase and Eiane (2007), with some modifications for *C. glacialis* and *C. hyperboreus* CI-CIII based on size distribution analysis (Appendix A), and the prosome length distribution in Ashijan et al. (2003) (Table 3). The filtration efficiency was assumed to be 100% when calculating the zooplankton abundance (ind.m^{-3}). All species names in this study is in accordance with WoRMS, World Register of Marine species (WoRMS Editorial Board, 2017).

Table 3 Length classification of the different copepodite stages of *C. finmarchicus, C. glacialis* and *C. hyperboreus*. Table from Daase and Eiana (2007), with modifications for *C. glacialis* and *C. hyperboreus* CI-CIII, based on own measurements and Ashijan et al. (2003).

Stage	PL (µm)		
	Calanus finmarchicus	*Calanus glacialis*	*Calanus hyperboreus*
CI	< 810	810 – 1000	> 1000
CII	< 1170	1170 – 1625	> 1625
CIII	< 1470	1470 – 2250	> 2250
CIV	< 2010	2010 – 2910	
CV	< 2900	> 2900	
AF	< 2950	> 2950	

Explanatory plots to show the development of the zooplankton community were created using Rstudio 1.0.136 (R Core Team, 2016). Redundancy analysis (RDA), a multivariate form of regression analysis available in CANOCO 4.5 for Windows (ter Braakand and Smilauer, 2002) was used to explore the zooplankton community composition and to relate it to potential explanatory variables. The RDA was performed on log x + 0.1 transformed zooplankton abundance data and non-transformed explanatory data. Only the significantly explanatory variables (Monte Carlo Permutation Test) were chosen. The Monte Carlo Permutation Test was run with 999 random permutations among whole plots containing the triplicates (i.e. split-plot design; ter Braak and Smilauer, 2002). Since there were no replicate zooplankton community data from station VMF 9, data from this station was made supplementary in the analysis. The Chl-*a* data were used as background environmental data for the zooplankton analyzes with CANOCO 4.5 for Windows (ter Braak and Smilauer, 2002), together with average temperature and salinity at the different stations, and Julian day.

2.4.3 Biomass analysis

The frozen samples were left overnight to thaw in the lab. The samples were then briefly rinsed with distilled water to remove any excess salt, and put into pre-weighed plastic trays. These were dried at 60ºC for 24 hours. During the sampling in July and August, distilled water was brought along on the boat, and the samples could therefore be put directly into trays before freezing. After drying, the trays with the dried samples were weighed again to determine weight of the sample by subtracting the weight of the empty tray. The weight was then transformed into dry weight per cubic of water (mg m^{-3}).

2.4.4 Analysis of egg incubation data

After ending the experiments, the AF were photographed alive using a stereomicroscope with a mounted camera. The image analysis program “imageJ” (Rasband, 2011) was used to measure the length of the AF, as well as the area of the lipid sac and the area of the body of the animal, to calculate lipid to body mass ratio according to Vogedes et al. (2010).

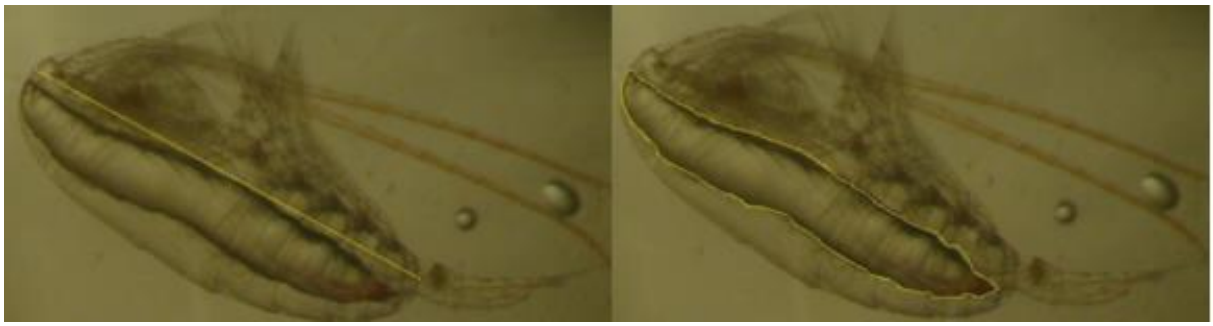

Figure 6 Measurement of prosome length (PL) and lipid sac area of *Calanus* spp. AF using "imageJ" (Rasband, 2011).

The AF were then put into cryotubes and frozen at -80ºC and kept at UNIS. The eggs in each cup were counted under the stereomicroscope, and then kept in the sea water lab at UNIS at 3ºC to 4ºC for approximately one week. The numbers of nauplii were counted to calculate the egg hatching success.

3.0 Results

3.1 Physical and biological environmental conditions

The mooring data collected at 12 m (Fig. 7a) and 68 m (Fig. 7b) show that changes in TS characteristics were most pronounced in the surface layer. The TS data points have an almost circular shape, indicating a seasonal component to the change in water properties. After the end of the winter cooling (May), the CTD profiles shown in Figure 7 were aligned with the time evolution of the mooring profile, which may indicate that downward mixing of the warm and fresher surface layer is the main component in shaping the water column during summer and autumn. The exception was vMF 1(green) in June, where the water column had a colder and fresher characteristic. At vMF 2 (black) on the other hand, the profile follows the mooring shape again, indicating advection that reached vMF1 in June, but not the very closely located mooring site (Fig. 3).

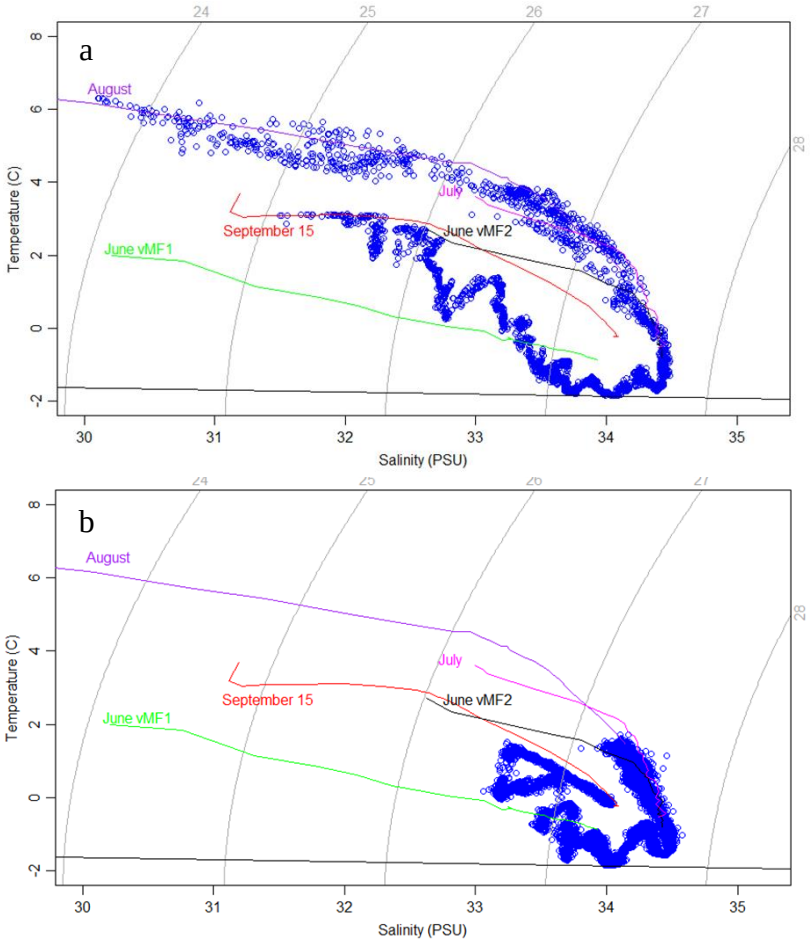

Figure 7 TS plot from the mooring data at 12 m (a) and 68 m (b) showing the annual development in salinity and temperature at these depths. CTD profiles from vMF 1 are shown in color, with the addition of the vMF 2 profile (black) from June. Black straight lines indicate freezing temperature.

The time series of temperature and salinity from the mooring at 12 m and 68 m indicate that there have been three major events of AW influx before in the inner part of the fjord when ice free, and one after the ice cover formed (Fig. 8). The rapid decrease in temperature before each influx can be explained by looking at the density at 12 m and 68 m. At the areas marked with red lines in Figure 8, the density throughout the water column was constant, making the water column unstable (Appendix B). This resulted in an overturning of the water column, lowering the temperature at depth (convection driven by heat loss through the surface). The steady increase in salinity throughout the winter can partly be explained by this AW/TAW influx, but also from brine release due to sea ice formation.

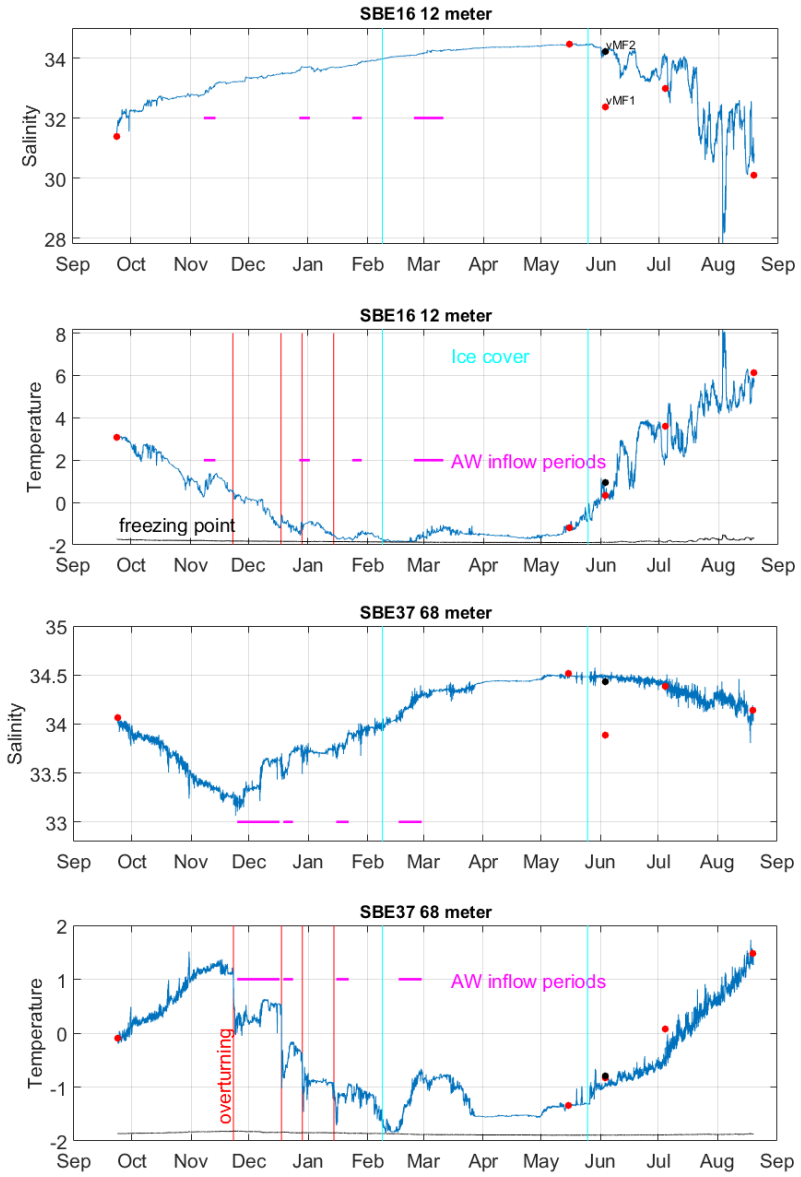

Figure 8 Time series of salinity and temperature at 12 m and 68 m. AW/TAW inflow periods are marked with pink. Overturning events with mixing of the water column is marked with red lines. Cyan lines indicate the period of ice cover. The red dots indicate the points in time where the CTD profiles from figure 7 were taken, and the black dot is the vMF 2 CTD, shown above the abnormal vMF 1 CTD in June.

Throughout the period with mooring measurements, the current at the mooring site was predominantly north westerly at all depths (Appendix C). In the top 30m, there were periods of a more westerly component, while the deeper layers were dominated by more eddy like current patterns.

The water column throughout the fjord changed from a warm and less saline situation in September 2015, to a colder and saline winter situation by April 2016. The CTD profiles from the sampling at vMF X and vMF Y (Appendix D) in March and mid-April show the same pattern as the profile from the ice edge at the end of April (Fig. 9). From June onwards, the water column gradually became warmer, and less saline as heat and meltwater from the fresh SW was mixed down into the water column. The water mass outside the fjord was warmer and more saline than inside the fjord throughout the entire study period. The June CTD profile of vMF 1 in the TS plot (Fig. 7) showed lower salinity than the mooring, which is also evident from the June transect in Figure 9, where the effect of a freshwater pool reaches down all the way to the bottom at the innermost station (vMF 1).

Chl-*a* analysis and fluorescence readings were not recorded in September 2015. In March and April at vMF X and vMF Y fluorescence readings at the CTD profiles were low (Appendix D). A fluorescence maximum was recorded at vMF 4 during sampling on 30th April 2016. Values were high in May as well, but remained low during the rest of the sampling period (Fig. 9). Integrated Chl-*a* measurements from the water samples were available for the 30th April – 1st May sampling, the June sampling, and for vMF 1 in July (no data from the other stations in July) (Appendix E). High values were recorded in May and June, but low values were recorded for vMF 1 in July.

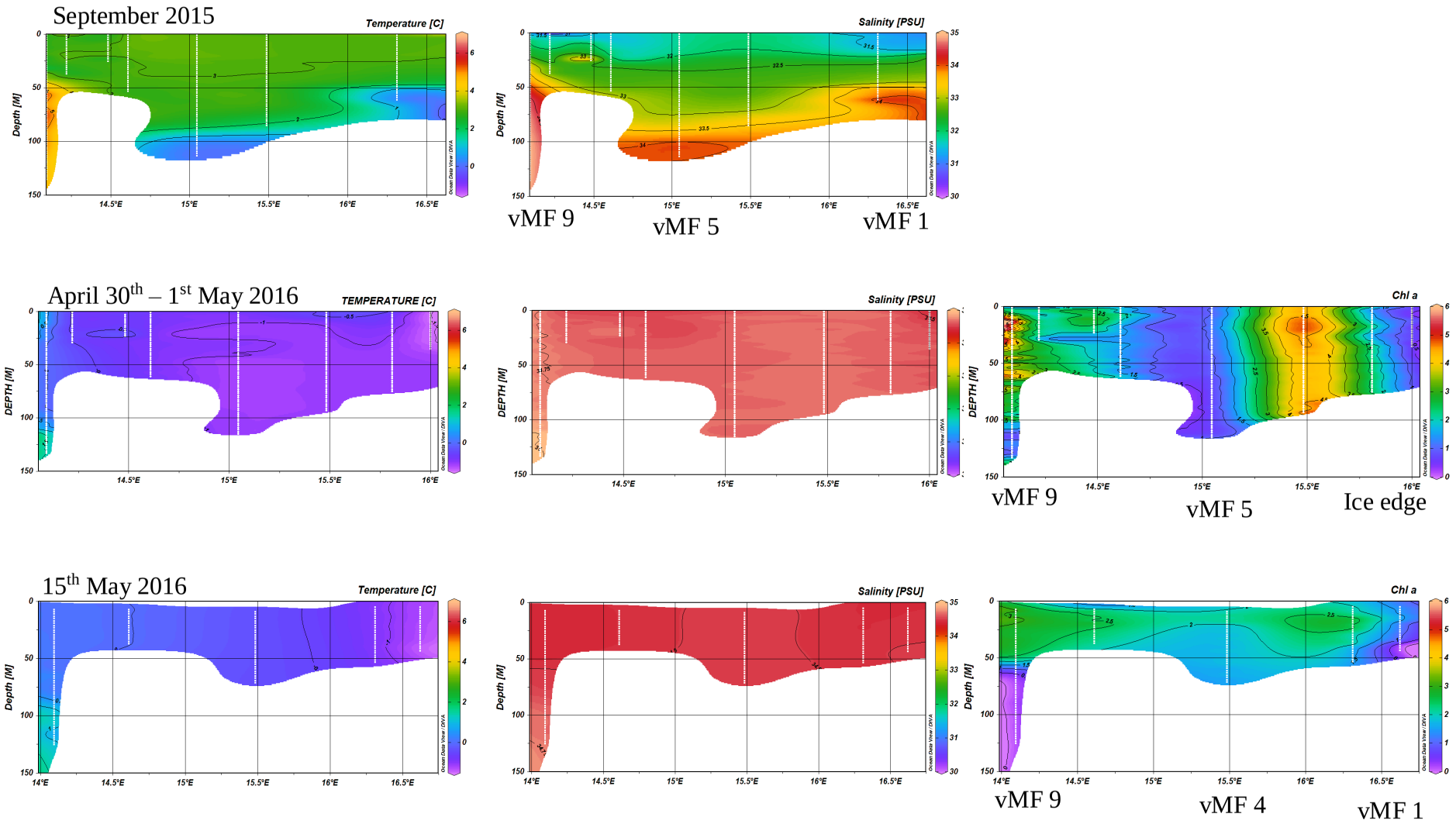

Figure 9 CTD profiles from the transect made every month, showing temperature (ºC), salinity (PSU) and fluorescence configured to measure Chl-*a* (ug l^{-1}).

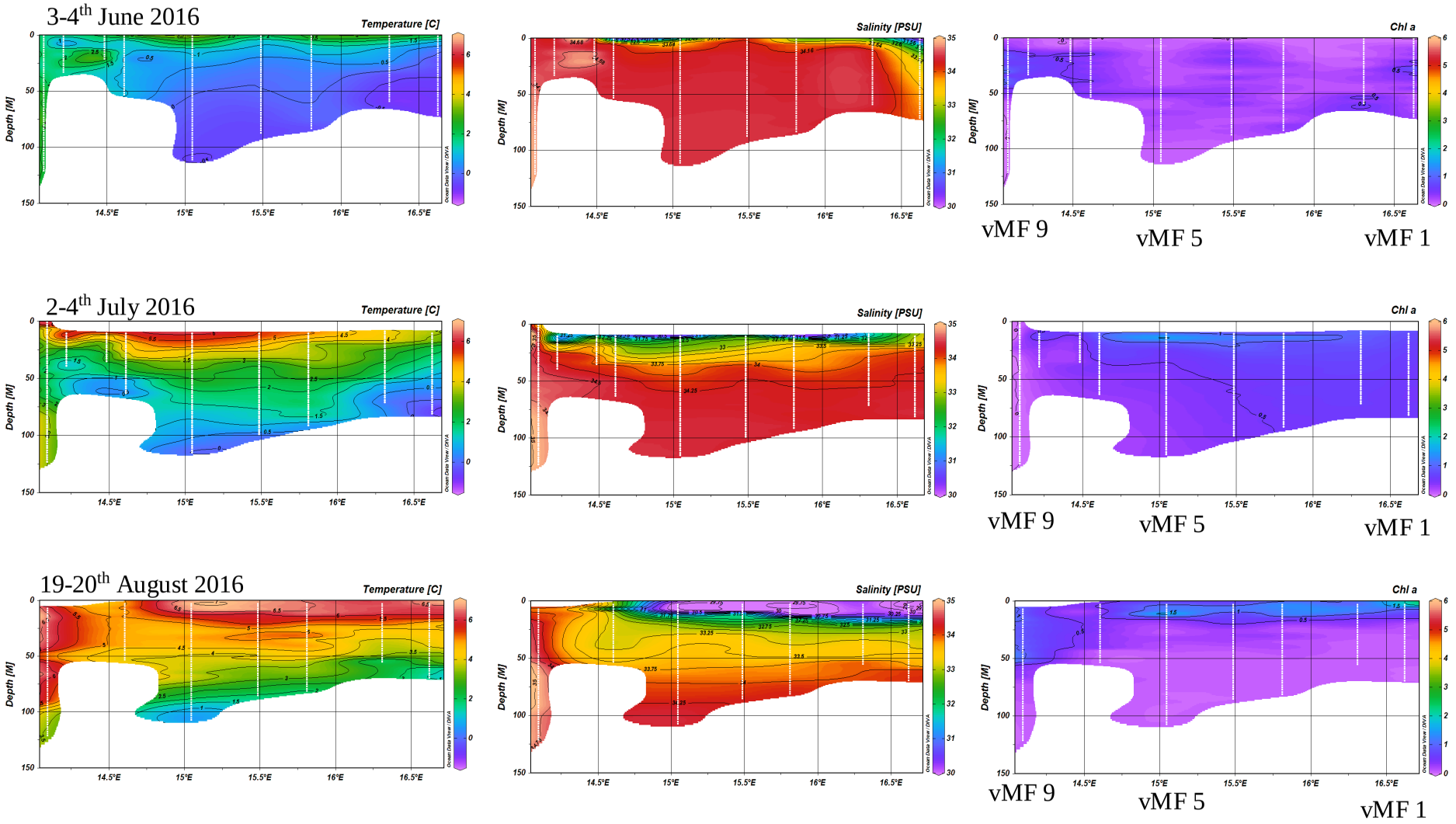

Figure 9 cont. CTD profiles from the transect made every month, showing temperature (ºC), salinity (PSU) and fluorescence configured to measure Chl-*a* (ug l^{-1}).

3.2 Zooplankton data

3.2.1 Total zooplankton community

In total 14 higher phyla and 21 taxa were found throughout the study period (Appendix F). In general, abundance was low during winter-spring (~600 ind. m^{-3}), and increased from May until maximum numbers (~20.000-57.000 ind. m^{-3}) were reached in August (Fig. 10). Abundance inside the fjord was higher than outside the fjord (vMF 9) on all sampling trips, but the species composition remained the same (Fig 10, Fig. 11). In June, the abundance was higher at vMF 1 than at vMF 5, however this pattern had reversed by July (Fig. 10). The low zooplankton abundance inside the fjord in September 2015 and 15th May 2016 may have been a result of the coarser mesh size (200µm) used these dates.

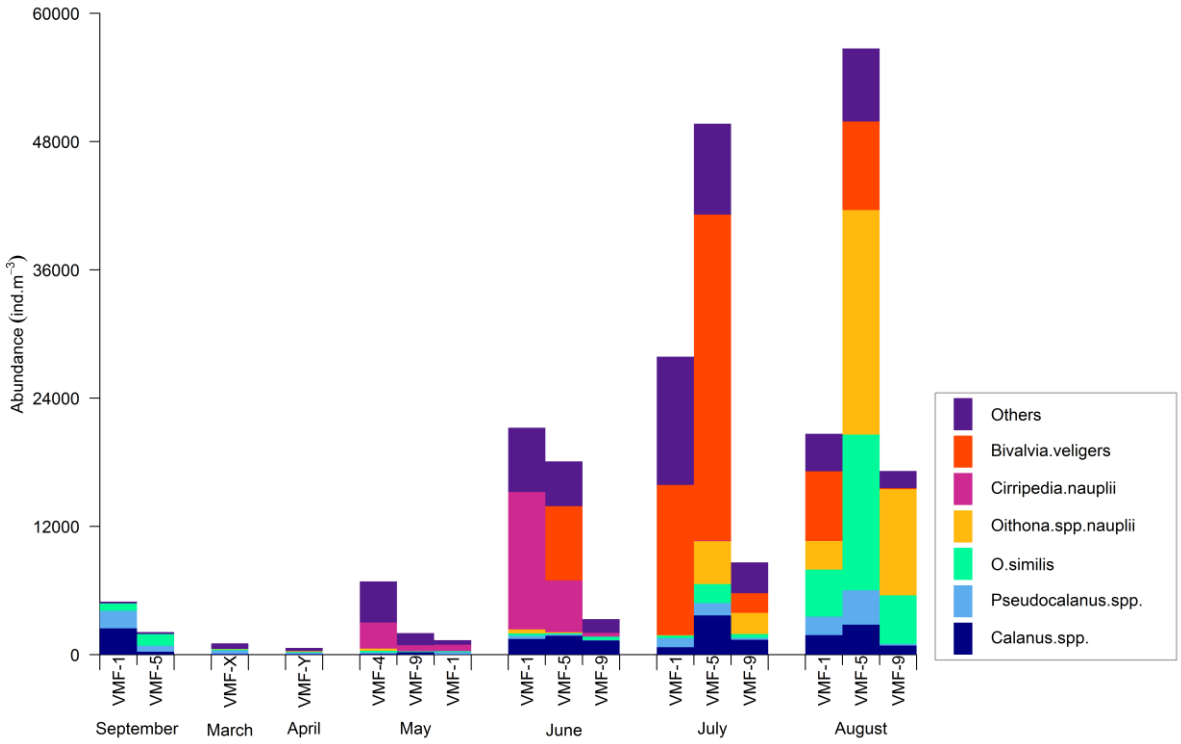

Figure 10 Overview of total abundance at the difference stations throughout the study period. Main constituents shown, groups that contribute less to total abundance are grouped in the category "others". The abundances are an average calculated from three replicates, based on the sum of bottom-20m and 20-0m samples, except for vMF 9, where one sample (bottom-20m + 20-0m) per station was analyzed. See Appendix F for full species list. See Table 2 for station information, and Table 3 for sampling information.

The holoplankton community was dominated mainly by the calanoid copepods *Calanus* spp. and *Pseudocalanus* spp., as well as the cyclopoid copepod *O. similis*. Peak zooplankton abundance was particularly related to high numbers of meroplankton, but also high abundances of eggs and nauplii (Fig. 10). In March, Polychaete larvae and *Pseudocalanus* spp. comprised roughly half (55.6%) of the community. Cirripedia nauplii started to increase in the end of April. The community at vMF 4 was dominated in equal parts by eggs (~2500

ind. m^{-3}) and Cirripedia nauplii (~2400 ind. m^{-3}), together accounting for 72.5% of the total zooplankton abundance, followed by copepod nauplii from calanoid copepods and *O. similis*. Cirripedia nauplii reached peak abundances (~12900 ind. m^{-3}) in June at vMF 1 (60.1% of the total abundance). The peak in Bivalvia veligers was reached in July (~14000 ind. m^{-3}at vMF 1 and ~30500 ind. m^{-3} at vMF 5) where they alone comprised half of the total zooplankton abundance (50.3% at vMF 1 and 61.4% at vMF 5). Ostracods was also numerous in July. In August *O. similis* and their nauplii (34.3%) together with Bivalvia veligers and Appendicularians dominated the community.

Other copepods found were *Metridia longa*, *Microcalanus* spp., *Triconia borealis, Acartia* spp. and *Microsetella norvegica*. Chaetognaths were present in all samples, and two species were found during this study, *Parasagitta elegans* and the much less abundant *Eukrhonia hamata*. In general, the abundance was low (<10 ind. m^{-3}), but with higher abundance (>15 ind. m^{-3}) in June and August, with a peak at vMF 5 in July. Among the most common macro zooplankton found, was *Thysanoessa inermis* and *Themisto abyssorum*, but only in low abundances (Appendix F).

3.2.2 Zooplankton-environment relationships

The two-dimensional RDA plot showed 54.1% of the total (100%) variability in the zooplankton community data (Fig. 11). The environmental variables temperature × fluorescence in the top 20 m, the integrated Chl-*a* biomass, salinity × temperature in the top 20m, Julian day and fluorescence alone in the upper 20m, together explained 67.3% of the total zooplankton community variability (Table 4), of which 43.3% were shown in the two-dimensional plot (Fig. 11).

Two strong gradients were seen in the zooplankton community composition. The first and strongest gradient along the x axis that was correlated with the seasonal development of the community from winter to summer. This gradient was 82% correlated with temperature × fluorescence at 0-20m. All replicates within each month clustered well together, following a slightly circular shape, which support a seasonal development in the zooplankton community composition that eventually reach the starting point again (Fig. 11). The second gradient likely represents a gradient within the productive season and the amount of food during this season (Fig. 11). The zooplankton community develops through the summer, and by looking at the integrated Chl-*a* (Appendix E) and temperature arrows in Figure 11, the gradient show

changes in conditions from early to late summer; from low to higher temperature, and high to lower Chl-*a* concentrations.

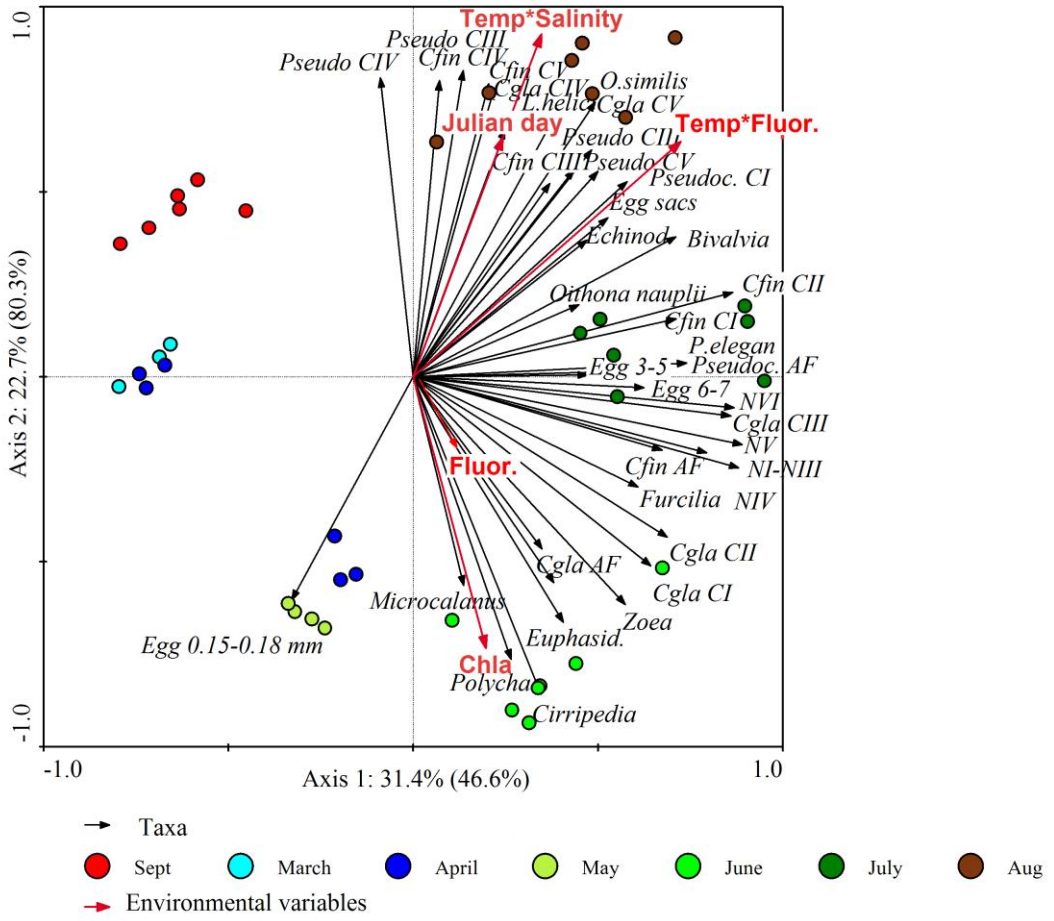

Figure 11 Ordination plot of the redundancy analyses (RDA), relating the variability in the zooplankton community to chosen significant (Monte Carlo Permutation test) environmental variables (Table 4).

Table 4 Ranking of the environmental variables (Monte Carlo Permutation test in the performed RDA) that best explained the variability in the zooplankton community composition in Van Mijenfjorden 2015-2016. The environmental variable that best explain the zooplankton community variability is ranked first, remaining variables are ranked on basis of additional fit. The environmental correlations to Axis 1 and 2 are also given.

	Expl. (%)	p-value	*f*	Axis 1	Axis 2
Temperature x Fluorescence (0 – 20m)	25.4	0.001	11.558	0.82	0.33
Chl-*a* integrated	18.1	0.006	10.532	0.00	-0.75
Salinity x Temperature (0 – 20m)	11	0.004	7.706	0.79	0.40
Julian day	7.5	0.006	6.072	0.36	0.56
Fluorescence (0 – 20m)	5	0.009	5.019	0.13	-0.28
Sum overall	67.3	0.001	8.769		

3.2.3 Biomass

The zooplankton biomass was lowest in April, increasing over summer with maximum values in August (Table 5). In June, there was a peak at vMF 1 (233.68mg m^{-3}), but the biomass was low at vMF 5 (42.57 mg m^{-3}). The same pattern can be seen in July, where there is a peak at vMF 5 (113.87 ±50.62 mg m^{-3}), while there are lower values at vMF 1 (63.71 ±8.02 mg m^{-3}) and vMF 9 (45.20 ±5.59 mg m^{-3}). In August, the biomass is higher than the previous months at both stations.

Table 5 Showing biomass in mg m^{-3} with standard deviation where applicable, from April 2016 to August 2016, over the whole water column (n=1). • n=2, * n=3.

Date	AB330	vMF 1	vMF3	vMF4	vMF5	vMF9
14.04.16	7.30 ±0.85*	-	-	-	-	-
30.04. – 01.05.16	-	-	10.50	15.10 ±2.96*	-	18.85
03.– 04.06. 16	-	233.68	-	-	42.57*	-
02.– 04.07.16	-	63.71 ±8.02*	-	-	113.87 ±50.62•	45.20 ±5.59•
19.– 20.08.16	-	271.03	-	-	205.68	-

3.2.4 Calanus spp.

The *Calanus* spp. population consisted of *C. glacialis, C. finmarchicus*, and very low abundances of *C. hyperboreus*. *C. glacialis* was more numerous than *C. finmarchicus* throughout the study period (Fig. 12). Reproduction started in April for *C. glacialis* and late May/early June for *C. finmarchicus*, and by August both populations primarily consisted of the overwintering stages. AM were only present in the samples at vMF 4 30th April and vMF 5 in June.

The highest abundance of *Calanus* spp. in September 2015 was found at vMF 1, where *C. glacialis* accounted for 83.5% of the *Calanus* spp. population (Fig. 12). In September, the dominating stage for *C. glacialis* was CIV (72% at vMF 1 and 69.7 % at vMF5), followed by CV. At vMF 1, only stage CIII-CV was present for *C. glacialis*, while at vMF 5 CII was also present. For *C. finmarchicus*, CV was the dominating stage (78.9% at vMF 1 and 68.8% at vMF 5), and all copepodite stages were present.

Abundance decreased during winter. The lowest abundance for this study was recorded in mid-April, with *C. glacialis* (44.0 ± 22.1 ind. m^{-3}) being more numerous than *C. finmarchicus* (6.2 ± 2.1 ind. m^{-3}). CIV - CV was still the dominant stages, but AF started to increase from

April (39.6% for *C. glacialis* and 42.2% for *C. finmarchicus* at vMF 4). At vMF 9 1st May, abundance was higher than inside the fjord, which is the only occasion this was recorded during this study. The population was also dominated by AF outside the fjord but not inside (*C. glacialis* 59.1% AF, *C. finmarchicus* 85.3% AF). The abundance increased from June onwards, and the stage composition changed (Fig. 12). Abundance at vMF 5 was higher than at vMF 1 for both species throughout the summer and autumn. Copepodite stages CI and CII were the dominant stages for both species in June, which agrees with the reproduction of the species during this time (Table 6). The highest abundance recorded in this study was at vMF 5 in July, with 2307.0 ± 777.0 ind. m^{-3} for *C. glacialis*, and 1371.2 ± 201.3 ind. m^{-3} for *C. finmarchicus*. The *C. finmarchicus* population was still dominated by smaller stages (CI-CII) in July, while for *C. glacialis*, CIII and CIV were the dominant stages. The last sampling took place in the beginning of August, and all stages were present except AM. Both species were again dominated by their overwintering stages. *C. glacialis* had an overweight of CIV, while *C. finmarchicus* seemed to prefer to overwinter as CV (Fig. 12).

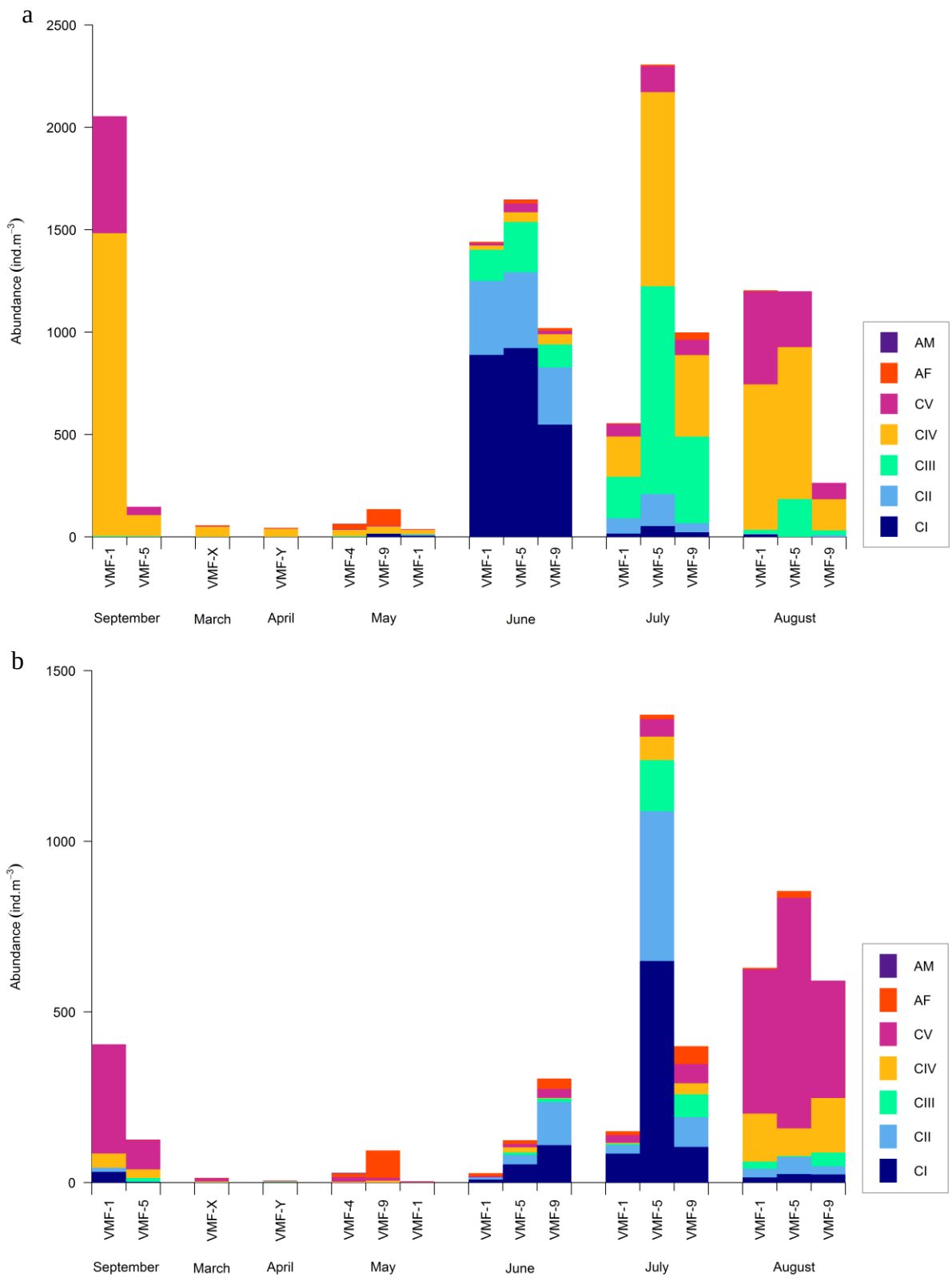

Figure 12 Bar plot showing the stage composition and abundance of *C. glacialis* (a) and *C. finmarchicus* (b) throughout the study period. The abundances are an average calculated from three replicates, based on the sum of bottom – 20 m and 20 – 0 m samples, except for vMF 9, where one sample (bottom – 20 m + 20 – 0 m) per station was analyzed. Notice that the x-axis in plot a and b does not have equal scales. For station and sampling info see Table 1 and 2.

3.2.5 Egg incubations

C. finmarchicus AF were not found in the samples until June, and thus only incubated in June, July and August (Table 6). From June onwards, the presence of *C. glacialis* AF decreased. In addition, the incubations were done on the boat from May onwards, and due to rough weather on the way back from Van Mijenfjorden in June, almost all the incubation cups were destroyed. As a consequence, the data presented for June is limited.

The egg production rate (EPR) was highest in May for *C. glacialis* (77.1 ±28.6), as was the hatching success (77.84 ±21.43) (Table 6). It is likely to believe that *C. glacialis* production had its peak somewhere between mid-April and mid-May, as the values before and after were lower. *C. finmarchicus* had the highest egg production rate in June (14.40 ±16.20), while the greatest hatching success was in July (76.88 ±13.28).

Table 6 Egg incubations for *C. glacialis* and *C. finmarchicus*. N - number of AF incubated. EPR – Egg production rate per day. TL- total lipids. The lipid content is calculated according to Vogedes et al. (2010). • N= 22, *N= 21.

	Station	Date	*N*	Egg laying AF (%)	EPR	Hatching success (%)	TL	Lipidsac % of body
	vMF 1	15. Apr	26	11.54	1.96 ±6.40	-	0.05 ±0.03	19.26 ±5.10•
	vMF 5	01. May	28	96.40	77.07 ±28.61	77.84 ±21.43	-	-
C. glacialis	vMF 1&5	4-5. Jun	7	85.71	10.47 ±12.75	19.96 ±19.14	0.07 ±0.03	26.41 ±8.19
	vMF 1&5	05. Jul	11	0.00	0.00	0.00	0.13 ±0.05	38.84 ±10.80
	vMF 1&5	18. Aug	4	25.00	3.74 ±7.48	0.00	-	-
	vMF 1&5	4-5. Jun	10	70.00	14.40 ±16.20	39.72 ±38.14	0.03 ±0.02	19.42 ±8.79
C. finmarchicus	vMF 1&5	05. Jul	47	14.89	3.29 ±8.70	76.88 ±13.28	0.05 ±0.03	27.01 ±8.65*
	vMF 1&5	18. Aug	31	22.58	3.10 ±7.57	54.27 ±28.89	-	-

The lipid content of the copepods increased from April to July (Table 6). In May, it was impossible to determine lipid content of *C. glacialis* as the females were full of eggs, and the lipid sac was not visible on the pictures used for analyzes. The pictures from August were not good enough to be able to see the lipid sac properly.

3.2.6 Pseudocalanus spp.

As seen in Figure 13, abundance of *Pseudocalanus* spp. decreased from September 2015 to April 2016. The lowest abundance was recorded at vMF 4 30th April (120.42±33.56 ind. m^{-3}). Abundance outside the fjord was continuously lower than inside the fjord. In September 2015, the abundance was highest in the inner part of the fjord (vMF 1). The dominant stages were CIII and CIV, accounting for 89% of the population at vMF 1, and 71% at vMF 5. The same stage composition was visible in March, where CIII and CIV accounted for 85.5% of population. The population developed to be dominated by older stages by mid – April (CIV-CV 73.6% of population), and by CV and AF at the end of April. An increase in AF were visible from mid – May, where AF accounted for 64.5% of the population. Stage CI and CII were not present in the samples in May, however the net from May 15th was 200µm, which does not sample the smaller stages representatively. All stages were present in June. An increase in abundance was visible from July and onwards at all stations. The population was

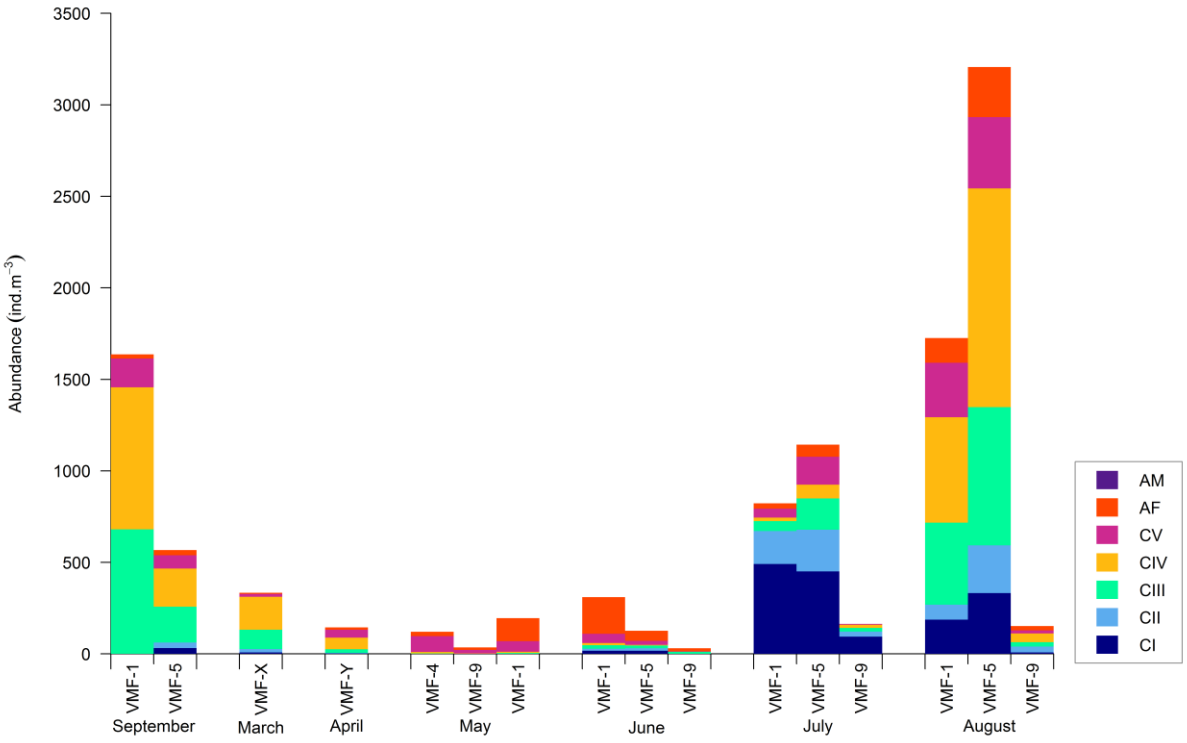

Figure 13 Bar plot showing the development and abundance of the *Pseudocalanus* spp. community. The abundances are an average calculated from three replicates, based on the sum of bottom – 20 m and 20 – 0 m samples, except for vMF 9, where one sample (bottom – 20 m + 20 – 0 m) per month was analyzed.

dominated by the smaller copepodite stages CI – CIII. The highest abundance was recorded in August, at vMF 5 (3206.5 ± 870.8 ind. m^{-3}), where the older stages (CIII-CV) again dominated the population.

3.2.7 Egg and nauplii

In June and July, eggs and nauplii contributed greatly to the total zooplankton abundance (Fig. 14), indicating that these months are important reproductive months. The results from June are based on the two nets sampled with 64µm. The largest eggs were present in the water column in March and April (0.38-0.45mm). These were most likely eggs of Chaetognaths (J. E. Søreide Pers Comm.). Eggs with a diameter of 0.15-0.18mm were abundant from April until June, and corresponds to the egg production of *Calanus* spp. (Table 6). Smaller nauplii stages were also abundant from June onwards, which agrees with the *Calanus* spp. reproduction. High abundance of small eggs (0.08-0.13mm) in the water column from June onwards, may suggest reproduction of *Pseudocalanus* spp. as AF were abundant in June, and small copepodite stages were present from July (Fig. 13). Egg sacs were present mostly in July and August. These belong to *O. similis*, which were abundant at this time (Fig. 10), and is also supported by the high abundance of *O. similis* nauplii.

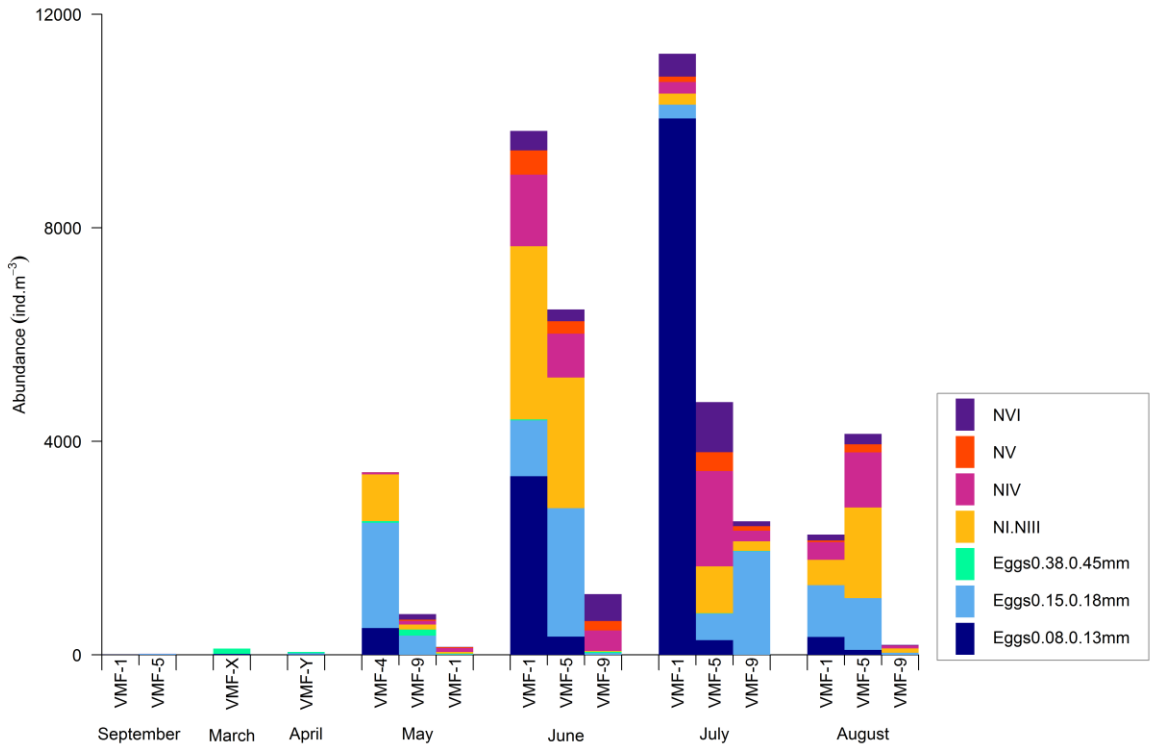

Figure 14 Bar plot of egg and nauplii abundances throughout the study period. The abundances are based on averages calculated from triplicates, based on the sum of bottom – 20 m and 20 – 0 m samples, except for vMF 9, where one sample (bottom – 20 m + 20 – 0 m) per month was analyzed, and June, where only the 64 µm net sample was used.

4.0 Discussion

4.1 Physical drivers and their influence on the zooplankton community abundance

The impact of advection is greater in fjords with a large ratio between the cross-sectional area of the mouth of the fjord, and the volume of the fjord (A/V ratio) (Aksnes et al., 1989). The A/V ratio for Van Mijenfjorden is in the order of $10^{-7}m^{-1}$, which is three magnitudes smaller than Kongsfjorden (A/V $10^{-4}m^{-1}$) (V. Tverberg Pers Comm.). The impact of AW/TAW advection can therefore be expected to be smaller in Van Mijenfjorden compared to other more open fjords such as Kongsfjorden and Isfjorden. However, even though Van Mijenfjorden has a narrow and shallow entrance, AW/TAW influences the fjord. The data from the mooring showed several influxes of AW/TAW between November 2015 and April 2016 (Fig. 8). In Kongsfjorden and Isfjorden which have no sills, AW/TAW can enter freely by topographic steering when the conditions are right (Cottier et al., 2005, Nilsen et al., 2008). This means the AW/TAW water must enter Van Mijenfjorden through different processes, and the tide seems to be the main entry mechanism for AW/TAW in Van Mijenfjorden. This is supported by Aksnes et al. (1989) that states that the most important exchange process for fjords with a shallow sill is the tide.

After entering the fjord, the AW/TAW is most likely distributed within the outer and inner basin by the currents created by the internal Kelvin waves (Skarðhamar and Svendsen, 2010, Støylen and Fer, 2014), and mixed with the LW present in the basin, by the breaking of these waves. Convective overturning, which happened several times during the winter also contributes to mixing (Fig. 8). In July and August, the downward mixing and distribution of heat in the water column reaches further down in the outer basin than in the inner basin (Fig. 9). As the energy in the Kelvin waves dissipate on their way around the fjord (Støylen and Fer, 2014), it may result in the outer basin being more thoroughly mixed than the inner basin.

The main influx that we observed in Van Mijenfjorden was in winter, while there was no clear recorded influx in summer. The fact that the influx is only visible at the mooring site in winter might be because the temperature in the water column is low, which will make the higher temperature signature of AW/TAW more visible. However, influx may happen also during summer, even though that there are no clear recordings of AW/TAW signatures. During the stratified conditions in summer, the internal Kelvin waves are more likely to break and cause mixing, which could cause the inflowing water to be mixed completely with the fjord water by the time it reaches the mooring placed in the innermost basin of the fjord. The increase in *C. finmarchicus* in Van Mijenfjorden in July however, may suggest some influx

from the shelf outside in June, when concentrations where also high outside the fjord at vMF 9.

No zooplankton data were sampled in the period from September to March. Although the mooring showed evidence of AW/TAW influx during this period, it is unlikely that the winter influxes of AW/TAW were rich in zooplankton, since the majority of the zooplankton remains at depth, or have low numbers in winter (Kosobokova, 1999, Halsband and Hirche, 2001, Stübner et al., 2016). The abundance decrease from September 2015 to April 2016 was most likely due to mortality being larger than influx. It is uncertain if *Calanus* spp. are able to have sustainable populations in the fjord. Almost no *Calanus* spp. were found during sampling in the inner basin in May 2014 (J. E. Søreide Pers. Comm), which indicate that the population is dependent on "supplies" from the shelf outside. The *Calanus* spp. found in March 2016 is likely the remnants of *Calanus* spp. that was advected into the fjord in September 2015. *C. glacialis* represented the majority of the *Calanus* spp. population in March and April 2016, suggesting that this species survive the winter better in the Arctic conditions in Van Mijenfjorden.

In summer, food is available in the surface layer, causing increased abundance in the top layers of the water column (Cottier at al., 2006, Falk-Petersen et al., 2009). However, there was no clear difference in the zooplankton abundance in the top 20 m and 20 m – bottom in the samples. During periods of midnight sun, unsynchronized vertical migration of zooplankton was found in Kongsfjorden, which also makes it difficult to pinpoint the position of the community in the water column (Cottier et al., 2006). The zooplankton community outside Van Mijenfjorden was therefore most likely distributed more evenly throughout the whole water column, meaning that part of the community would be subjected to advection with flooding tide, but the density of the influx would most likely not be very high. The zooplankton community switches back to a synchronized vertical migration from the middle of August, with the onset of dark and light periods (Cottier et al., 2006), which suggests that larger abundances of zooplankton can be advected into the fjord when darkness coincides with peak tidal inflow. A large influx event like this can explain the high *Calanus* spp. abundances in September 2015.

The high abundance found at vMF 5 from June to August might be an indication of advection, bringing zooplankton into the fjord, but this is not supported by the low abundance outside the fjord at vMF 9. Local processes within the fjord is more likely to be the cause of the increase. The main current in the fjord follow an eddy like flow pattern, inwards on the south side and

outwards on the north side, with stronger currents in the broad outer basin (Skarðhamar and Svendsen, 2010). This can cause zooplankton to be retained longer in the outer basin, creating a local eddy in the area around vMF 5, which again creates a biological hotspot within the basin. This may also be the reason for the local bloom event seen at vMF 4, very close to vMF 5 in April/May (Fig. 9).

Because of the consistently higher abundances inside the fjord versus outside, it is reasonable to believe that advection of zooplankton biomass into the fjord during this study was small. Local reproduction and population development inside the fjord seem to be the main driver for the zooplankton community structure and progression in Van Mijenfjorden 2016. However, the high abundance of *Calanus*. spp. in September 2015, was most likely due to advective processes, highlighting also the importance of influx from the shelf.

4.2 Biological drivers and their influence on the zooplankton community

4.2.1 Total zooplankton community composition

In spring, the total abundance was low, as was the biomass, with an increase towards autumn. This is also documented from Kongsfjorden and Isfjorden, where zooplankton abundance and biomass increases from spring to autumn (Walkusz et al., 2009, Stübner et al., 2016, Gluchowska et al., 2016). Over all, the abundance in this study was over five times that reported from Isfjorden and Kongsfjorden in 2002/2007 (Walkusz et al., 2009, Gluchowska et al., 2016). The mesh size in this study (64 µm) was smaller than that used in Kongsfjorden and Isfjorden (180 µm), and therefore smaller animals, like Bivalvia veligers, were captured resulting in higher abundance data. In a study by Stübner et al. (2016) in Isfjorden/Adventfjorden, using the same fine mesh size (64 µm), abundances were even greater (~92200 ind. m^{-3}) than those found in this study in Van Mijenfjorden (~20.000-57.000 ind. m^{-3}). The sampling interval was more frequent (one to three times per month) in Isfjorden/Adventfjorden, so there was a larger chance of capturing the meroplankton peaks in this study versus in mine.

The zooplankton increase in Van Mijenfjorden in June and July was largely due to very abundant meroplankton. During the study period, meroplankton had two distinct peaks, mainly comprising of two different taxa, Cirripedia nauplii in June, and Bivalvia veligers in July. Polychaeta larvae comprised a large part of the community in Van Mijenfjorden in March. The peaks in Cirripedia and Bivaliva both happened during the productive season, indicating that there is a strong seasonal dynamic in the meroplankton community. This is

also evident from the RDA analysis (Fig. 11), where two strong gradients were seen; one from fall/winter to summer and one during the productive summer season related to algal food availability. Cirripedia nauplii were strongly positively correlated to high values of Chl-*a* biomass. Cirripedia keep ready larvae in their brood chambers and release their nauplii directly into the water column when favorable feeding conditions appear (Crisp and Spencer, 1958). Bivalvia veligers occurred in peak abundances later in the season. Most Bivalves release gametes into the water column, and will not form a zygote before encountering another gamete. The larvae are therefore not caught in the zooplankton net until later in the season when it has developed to a large enough size.

In Van Mijenfjorden the peak in Cirripedia started earlier (mid-April) than in Isfjorden/Adventfjorden (end of April-beginning of May), while the same pattern was observed for Bivalvia veligers (beginning of June) (Stübner et al., 2016). However, the sampling resolution in this study was much lower than that of Stübner et al. (2016). The spring bloom was placed in the beginning of May in this study, and the same timing was recorded by Stübner et al. (2016), indicating that the same patterns found in Isfjorden/Adventfjorden is also present in Van Mijenfjorden. The same peak in meroplankton is not visible at vMF 9, which supports the argument that local processes is the dominant factor driving the zooplankton community succession in Van Mijenfjorden.

The three most abundant copepods were, in order, *O. similis, Calanus* spp.(mainly *C. glacialis*) and *Pseudocalanus* spp.. This is in accordance with studies done in more open fjords around Svalbard, like Isfjorden and Kongsfjorden (Walkusz et al., 2009, Gluchowska et al., 2016). However, which of these species that was most abundant at any given time varied throughout the study. In Van Mijenfjorden *Calanus* spp. dominated in September 2015 both at vMF 1 and vMF 5. In March and April 2016, *Pseudocalanus* spp. and *O. similis* were more abundant than *Calanus* spp. at all stations. In June, *Calanus* spp. was more than three times as abundant as *O. similis* and *Pseudocalanus* spp. both at vMF 1 and vMF 5, while in July, *Pseudocalanus* spp. was most numerous at vMF 1, and *Calanus* spp. at vMF 5. The copepod abundance was low compared to the presence of meroplankton and eggs and nauplii during the summer. However, in August *O. similis* and their nauplii was by far the most abundant species at both stations, followed by *Calanus* spp. at vMF 1 and by *Pseudocalanus* spp. at vMF 5. Outside the fjord, at vMF9, *Calanus* spp. was the dominant taxa in all months, except for in August, when *O. similis* dominated also here.

In Kongsfjorden in 2002 (Walkusz et al., 2009) and in 2007 (Gluchowska et al., 2016) *C. finmarchicus* was at times twice as abundant as *C. glacialis*, which is in strong contrast to Van Mijenfjorden, where *C. glacialis* was more abundant than *C. finmarchicus* during the entire study. This may be because of more AW/TAW influence in Kongsfjorden. This is supported by the high numbers of *C. glacialis* in relation to *C. finmarchicus* found in Rijpfjorden, which is more Arctic (Weydmann et al., 2013).

O. similis was the most abundant copepod found in this study, as it was in Kongsfjorden and Rijpfjorden as well (Walkusz et al., 2009, Weydmann et al., 2013, Gluchowska et al., 2016). However, peak abundances in Van Mijenfjorden (~4400-15000 ind. m^{-3}) was up to five times larger than those found in Kongsfjorden (Walkusz et al., 2009, Gluchowska et al., 2016). Rijpfjorden had peak abundance of 256189 ind. m^{-3}, which is significantly higher than in the fjords on the west side of Spitsbergen (Weydmann et al., 2013). In Van Mjenfjorden *Pseudocalanus* spp. was the third most abundant species (~1700-3200 ind. m^{-3}), while it was the second most abundant species in Rijpfjorden (peak abundance of 63697 ind. m^{-3}) (Weydmann et al., 2013). In Kongsfjorden abundances was roughly half of what was found in this study. This might be due to the coarser mesh size, which under-sample small copepodite stages of *Pseudocalanus* spp..

The community composition show similar patterns in Van Mijenfjorden as in the high Arctic Rijpfjorden, and in the more Atlantic influenced Kongsfjorden and Isfjorden. The different water masses that influence these fjords may be the cause of the huge difference in abundance. The more ArW in Rijpfjorden seem to contain higher abundances than the AW/TAW in Kongsfjorden. The intermediate abundances found in Van Mijenfjorden may indicate that the fjord is influenced by a mix in these water masses in addition to local water mass formation and process.

4.2.2 Reproduction and development

As seen in the RDA analysis (Fig. 11), the seasonal gradient captures the reproductive cycle and the stage development of the zooplankton community. In addition, the dominance of different copepods during different times of the year can also be explained partly by their reproductive cycle.

Overwintering stages (CIV-CV) of both *C. glacialis* and *C. finmarchicus* were present in the water column in September 2015 and March 2016, AF were also present from March. Both species reproduced in the fjord. *C. glacialis* had a peak in reproduction earlier than *C.*

finmarchicus, which is probably due to their ability to fuel reproduction by internal lipid reserves and utilize the ice algal bloom (Runge & Ingram, 1988, Hirche and Kattner, 1993, Falk-Petersen et al., 2009, Daase et al., 2013). The data most likely captured the peak of *C. glacialis* quite accurately to the beginning of May at vMF 5. There are no egg incubation data from vMF 1, but it corresponds well to the peak of CI in the beginning of June at all stations, and the high abundance of nauplii and eggs in the water column. This reflects the dominance of *Calanus* spp. in June at all stations. Egg production was lower both before and after at both vMF 1 and vMF 5. Egg production in June may have been higher, but due to rough seas, most of the egg incubations were lost in June and the estimates were done from a few females only. However, egg production was probably still lower in June than in May, as there was low abundance of AF in June, and low abundance of CI in July. Lipid content of *C. glacialis* also increased from June, which indicate that ingested food most likely fueled production. This was probably the case in May also, since the fjord was mostly ice free and a pelagic bloom was visible in the water column (Fig. 9).

C. finmarchicus coincide spawning with the phytoplankton bloom in The Barents Sea (Falk-Petersen et al., 2009), and Chl-*a* readings places the peak pelagic bloom sometime in the beginning of May in Van Mijenfjorden (Fig. 9), which corresponds well to production in late May, and increase in CI from June onwards. The highest abundance of CI was recorded in July at vMF 5, one month later than for *C. glacialis*. The increase at vMF 5 in July could also be an indication of an influx of water from outside the fjord, especially since there was an increase in AF. In Kongsfjorden, Basedow et al. (2004) argued that *C. finmarchicus* AF reproduced in the warmer AW/TAW on the shelf, and the small copepodite stages were then advected into the fjord. Lipid content of the *C. finmarchicus* AF were lower than in *C. glacialis* AF, which might be explained by their smaller size.

The *Calanus* spp. egg production in Van Mijenfjorden was later than previously recorded from Kongsfjorden, where CI and CII of *C. glacialis* dominated the last weeks of May, and earlier than Rijpfjorden, where young stages peaked in July (Daase et al., 2013). Also, the phytoplankton bloom in Kongsfjorden can be as early as April, while it peaked as late as in July in Rijpfjorden (Daase et al., 2013). The placement of the peak phytoplankton bloom in the beginning of May in Van Mijenfjorden, places the production in between the other two fjords. As Kongsfjorden is open and display more Atlantic characteristics compared to the Arctic signature of Rijpfjorden, Van Mijenfjorden seem to be a fjord with mixed properties,

which is reflected in the succession in *C. glacialis* being somewhere in the middle of the timing in the other two fjords.

By August, all stations were dominated by the overwintering stages (CIV-CV). *C. glacialis* were represented by a larger portion of CIV than CV, while *C. finmarchicus* mainly by CV. This suggests that *C. glacialis* may have a 1-2-year life cycle in Van Mijenfjorden, while *C. finmarchicus* has a 1 year life cycle (Falk-Petersen et al., 2009).

The presence of both species throughout the year may suggest that they are having sustainable populations within the fjord. This discovery might be special to the 2015/2016 winter. High abundances were found in September 2015 and in August 2016, which might indicate an influx of shelf waters bringing *Calanus* spp. into the fjord. This is supported by the low ice concentrations in the fjord during the winter (Fig. 4). In addition, *C. finmarchicus* had similar abundances outside the fjord as inside the fjord in August. Low abundances of *Calanus* spp. was found in 2014, and during the 2014/2015 winter the fjord was covered in ice, suggesting less influence of AW/TAW (Søreide Pers. Comm). This may indicate that 2016 was a special year regarding *Calanus* spp. In addition, *Calanus* spp. overwinter at depth, and Van Mijenfjorden may be too shallow (115m), as they have been known to descend to below 500m (Falk-Petersen et al., 2009).

Even though three different species of *Pseudocalanus* spp. are present in Svalbard; *P. acuspes, P. minutus and P. moultoni* (Frost, 1989, Aarbakke et al., 2011), it is reason to believe that *P. acuspes* was the dominant species in Van Mijenfjorden as the other two are more oceanic and abundance of *Pseudocalanus* spp. was higher inside the fjord (Lischka and Hagen, 2005, Aarbakke et al., 2011). The seasonal trend in the *Pseudocalanus* spp. population agrees well with other studies (Halsband and Hirche, 2001, Lischka and Hagen, 2005, Renz et al., 2007). Abundance was low in spring, and AF represented the main part of the population in May and June. The small copepodite stages (CI-CII) dominated the population in July, which explains the increase in *Pseudocalanus* spp. abundance in July, and places the reproduction a month later than for *C. glacialis*, and closer to *C. finmarchicus*. In August, the population was again dominated by the overwintering stages (CIII-CV) (Conover and Siferd, 1993). From these data, it is not possible to answer if there were any production during winter. Halsband and Hirche (2007) recorded production all year round except December and March in the North Sea, while Lischka and Hagen (2005) recorded production from May to June in Kongsfjorden. Since Van Mijenfjorden seem to be a more Arctic fjord than Kongsfjorden, any reproduction during winter would be very low if present at all.

O. similis was abundant during the entire study, but was the last of the dominant copepod species to reach a peak in reproduction. Egg sacs and large numbers of *Oithona* nauplii were present in the water column from July, and reached a peak in August, as did the copepodite abundance, which is the same timing reported for Kongsfjorden (Lischka and Hagen, 2005). The total dominance of *O. similis* is visible in the waters outside the fjord as well, particularly in August when abundances are high. This may be connected to the same advection that possibly transported *C. finmarchicus* into the fjord.

Both *Pseudocalanus* spp. and *O. similis* are omnivorous species, and therefor do not depend on the phytoplankton bloom in the same degree as *Calanus* spp. Their reproduction seems to be more correlated with warmer temperature later in the season (Fig. 11). If this is an autocorrelation, or an actual necessity for the species to reproduce in the fjord is not known, but studies have shown that reproduction increases, development time is shorter and survival higher with higher temperatures for *O. similis* (Ward and Hirst, 2007). *P. acuspes* overwinter as CIII-CV, and finish development in spring to AF/AM by use of ingested food (Conover and Siferd, 1993). This will also put the reproduction later in the season, and explain why we see a peak later in the year than for *Calanus* spp. that molts to AF during winter. The higher temperatures later in the season may be one of the reasons why their offspring is able to rapidly grow to the overwintering stages by August/September.

5.0 Conclusion

It is evident that Van Mijenfjorden is influenced by AW/TAW. To which extent, and if this process is significant throughout the entire year is more difficult to answer. The mooring at the fjord mouth was lost, which makes it hard to identify influxes during the summer since the water is heavily influenced by mixing before it reaches vMF 1. However, the development in the zooplankton community, in particularly the greater abundance of meroplankton inside the fjord compared to outside suggests that local processes was the main driving force for zooplankton community development and biomass increase. The only contradiction to this notion is the increase in *C. finmarchicus* and *O. similis* in July and August.

The zooplankton community in the fjord show the same structure and seasonal dynamic as communities from other fjords in Svalbard, like Kongsfjorden, Isfjorden and Rijpfjorden. The community is dominated by the same copepod species as these fjords; *Calanus* spp., *Pseudocalanus* spp. and *O. similis*. However, the timing in succession and reproduction falls between the heavily AW/TAW influenced Kongsfjorden and Isfjorden, and the Arctic Rijpfjorden, suggesting that the community in Van Mijenfjorden is influenced by a mix of these water masses and not as prolonged sea ice cover as Rijpfjorden.

From this study, it would seem that *C. glacialis* and *C. finmarchicus* both may have the potential to have reproductive sustainable populations in Van Mijenfjorden. The presence of both species in September 2015, and in March 2016 suggest that they have overwintered in the fjord. Both species were able to reproduce, but the reproductive success of *C. glacialis* was higher than that of *C. finmarchicus*. This suggest that *C. glacialis* are better adapted to the conditions within the fjord. However, previous data collected in the fjord have suggested very low abundances of *Calanus* spp., which the shallow depth of the fjord would support since it is less than the preferred depth for overwintering for these two species. A more plausible theory would then be that the small copepods, *Pseudocalanus* spp. and *O. similis* are present year-round, while the *Calanus* spp. population is able to overwinter, but is supplied by the influx of AW/TAW from the shelf.

References

Aarbakke, O. N. S., Bucklin, A., Halsband, C., & Norrbin, F. (2011). Discovery of *Pseudocalanus moultoni* (Frost, 1989) in Northeast Atlantic waters based on mitochondrial COI sequence variation. *Journal of Plankton Research, 33*(10), 1487-1495. doi:10.1093/plankt/fbr057

Aksnes, D. L., Aure, J., Kaartvedt, S., Magnesen, T., & Richard, J. (1989). Significance of advection for the carrying capacities of fjord populations. *Marine Ecology Progress Series, 50*(3), 263-274. doi:10.3354/meps050263

Ashjian, C. J., Campbell, R. G., Welch, H. E., Butler, M., & Van Keuren, D. (2003). Annual cycle in abundance, distribution, and size in relation to hydrography of important copepod species in the western Arctic Ocean. *Deep Sea Research Part I: Oceanographic Research Papers, 50*(10–11), 1235-1261. doi:http://dx.doi.org/10.1016/S0967-0637(03)00129-8

Bailey, J., Durbin, E. G., & Rynearson, T. (2016). Species composition and abundance of copepods in the morphologically cryptic genus *Pseudocalanus* in the Bering Sea. *Deep Sea Research Part II: Topical Studies in Oceanography, 134*, 173-180. doi:http://dx.doi.org/10.1016/j.dsr2.2015.04.017

Basedow, S. L., Eiane, K., Tverberg, V., & Spindler, M. (2004). Advection of zooplankton in an Arctic fjord (Kongsfjorden, Svalbard). *Estuarine Coastal and Shelf Science, 60*(1), 113-124. doi:10.1016/j.ecss.2003.12.004

Berge, J., Cottier, F., Varpe, O., Renaud, P. E., Falk-Petersen, S., Kwasniewski, S., . . . Majaneva, S. (2014). Arctic complexity: a case study on diel vertical migration of zooplankton. *Journal of Plankton Research, 36*(5), 1279-1297. doi:10.1093/plankt/fbu059

Blachowiak-Samolyk, K., Kwasniewski, S., Dmoch, K., Hop, H., & Falk-Petersen, S. (2007). Trophic structure of zooplankton in the Fram Strait in spring and autumn 2003. *Deep Sea Research Part II: Topical Studies in Oceanography, 54*(23–26), 2716-2728. doi:http://dx.doi.org/10.1016/j.dsr2.2007.08.004

Blachowiak-Samolyk, K., Søreide, J.E., Kwasniewski, S., Sundfjord, A., Hop, H., Falk-Petersen, S., and Hegseth, E.N. (2008). Hydrodynamic control of mesozooplankton abundance and biomass in northern Svalbard waters (79-81°N). Deep-Sea Research II *55*, 2210-2224.

ter Braak, C. J. F., and Smilauer, P. (2002). CANOCO reference manual and CanoDraw for Windows User's guide: Software for canonical community ordination (New York: Microcomputer Power).

Cleary, A. C., Durbin, E. G., Rynearson, T. A., & Bailey, J. (2016). Feeding by *Pseudocalanus* copepods in the Bering Sea: Trophic linkages and a potential mechanism of niche partitioning. *Deep-Sea Research Part Ii-Topical Studies in Oceanography, 134*, 181-189. doi:10.1016/j.dsr2.2015.04.001

Conover, R. J. (1988). Comparative life histories in the genera C*alanus* and *Neocalanus* in high-latitudes of the northern hemisphere. *Hydrobiologia, 167*, 127-142. doi:10.1007/bf00026299

Conover, R. J., & Siferd, T. D. (1993). Dark-Season Survival Strategies of Coastal Zone Zooplankton in the Canadian Arctic. *Arctic, 46*(4), 303-311.

Cottier, F., Tverberg, V., Inall, M., Svendsen, H., Nilsen, F., & Griffiths, C. (2005). Water mass modification in an Arctic fjord through cross-shelf exchange: The seasonal hydrography of Kongsfjorden, Svalbard. *Journal of Geophysical Research-Oceans, 110*(C12). doi:10.1029/2004jc002757

Cottier, F. R., Nilsen, F., Skogseth, R., Tverberg, V., Skardhamar, J., & Svendsen, H. (2010) Arctic fjords: A review of the oceanographic environment and dominant physical processes. *Vol. 344. Geological Society Special Publication* (pp. 35-50).

Cottier, F. R., Tarling, G. A., Wold, A., & Falk-Petersen, S. (2006). Unsynchronized and synchronized vertical migration of zooplankton in a high arctic fjord. *Limnology and Oceanography, 51*(6), 2586-2599.

Crisp, D.J. and Spencer, C. P. The control of the hatching process in barnacles. Proc. R. Soc. London B Biol. Sci 149, 278-299.

Daase, M., & Eiane, K. (2007). Mesozooplankton distribution in northern Svalbard waters in relation to hydrography. *Polar Biology, 30*(8), 969-981. doi:10.1007/s00300-007-0255-5

Daase, M., Falk-Petersen, S., Varpe, O., Darnis, G., Soreide, J. E., Wold, A., . . . Fortier, L. (2013). Timing of reproductive events in the marine copepod *Calanus glacialis*: a pan-Arctic perspective. *Canadian Journal of Fisheries and Aquatic Sciences, 70*(6), 871-884. doi:10.1139/cjfas-2012-0401

Falk-Petersen, S., Dahl, T. M., Scott, C. L., Sargent, J. R., Gulliksen, B., Kwasniewski, S., . . . Millar, R. M. (2002). Lipid biomarkers and trophic linkages between ctenophores and copepods in Svalbard waters. *Marine Ecology Progress Series, 227*, 187-194. doi:10.3354/meps227187

Falk-Petersen, S., Timofeev, S., Pavlov, V., and Sargent, J.R. (2007). Climate variability and the effect on Arctic food chains. The role of *Calanus*. In Arctic-Alpine ecosystems and people in a changing environment, J.R. Ørbæk, Tombre, T., Kallenborn, R, Hegseth, E., Falk-Petersen, S. Hoel, A. H., ed. (Berlin: Springer), pp. 147-166.

Falk-Petersen, S., Mayzaud, P., Kattner, G., & Sargent, J. (2009). Lipids and life strategy of Arctic *Calanus*. *Marine Biology Research, 5*(1), 18-39. doi:10.1080/17451000802512267

Fer, I., & Widell, K. (2007). Early spring turbulent mixing in an ice-covered Arctic fjord during transition to melting. *Continental Shelf Research, 27*(15), 1980-1999. doi:10.1016/j.csr.2007.04.003

Frost, B. W. (1989). A taxonomy of the marine calanoid copepod genus *Pseudocalanus*. *Canadian Journal of Zoology-Revue Canadienne De Zoologie, 67*(3), 525-551.

Gabrielsen, T. M., Merkel, B., Søreide, J. E., Johansson-Karlsson, E., Bailey, A., Vogedes, D., . . . Berge, J. (2012). Potential misidentifications of two climate indicator species of the marine arctic ecosystem: *Calanus glacialis* and *C. finmarchicus*. *Polar Biology, 35*(11), 1621-1628. doi:10.1007/s00300-012-1202-7

Gluchowska, M., Kwasniewski, S., Prominska, A., Olszewska, A., Goszczko, I., Falk-Petersen, S., . . . Weslawski, J. M. (2016). Zooplankton in Svalbard fjords on the Atlantic-Arctic boundary. *Polar Biology, 39*(10), 1785-1802. doi:10.1007/s00300-016-1991-1

Haarpaintner, J., Gascard, J. C., & Haugan, P. M. (2001). Ice production and brine formation in Storfjorden, Svalbard. *Journal of Geophysical Research-Oceans, 106*(C7), 14001-14013. doi:10.1029/1999jc000133

Halsband, C., & Hirche, H. J. (2001). Reproductive cycles of dominant calanoid copepods in the North Sea. *Marine Ecology Progress Series, 209*, 219-229. doi:10.3354/meps209219

Hanssen-Bauer, I., Solaas, M., & Steffensen, E. L. (1990). *The climate of Spitsbergen.* Norwegian Meteorological Institute, Oslo, Report 39/90.

Hirche, H. J., & Kattner, G. (1993). Egg-production and lipid-content of *Calanus glacialis* in spring: indication of a food-dependent and food-independent reproductive mode. *Marine Biology, 117*(4), 615-622. doi:10.1007/bf00349773

Hirche, H. J., & Kosobokova, K. (2007). Distribution of *Calanus finmarchicus* in the northern North Atlantic and Arctic Ocean - Expatriation and potential colonization. *Deep-Sea Research Part Ii-Topical Studies in Oceanography, 54*(23-26), 2729-2747. doi:10.1016/j.dsr2.2007.08.006

Hirche, H. J., & Kosobokova, K. N. (2011). Winter studies on zooplankton in Arctic seas: the Storfjord (Svalbard) and adjacent ice-covered Barents Sea. *Marine Biology, 158*(10), 2359-2376. doi:10.1007/s00227-011-1740-5

Holm-Hanssen, O and Riemann, B (1978) Chlorophyll a determination: improvements in methodology chlorophyll a determination: in methodology improvements, Oikos, 30, 438-447.

Ji, R. B., Ashjian, C. J., Campbell, R. G., Chen, C. S., Gao, G. P., Davis, C. S., . . . Beardsley, R. C. (2012). Life history and biogeography of *Calanus* copepods in the Arctic Ocean: An individual-based modeling study. *Progress in Oceanography, 96*(1), 40-56. doi:10.1016/j.pocean.2011.10.001

Johannessen, O. M., Bengtsson, L., Miles, M. W., Kuzmina, S. I., Semenov, V. A., Alekseev, G. V., . . . Cattle, A. P. (2004). Arctic climate change: observed and modelled temperature and sea-ice variability. *Tellus Series a-Dynamic Meteorology and Oceanography, 56*(4), 328-341. doi:10.1111/j.1600-0870.2004.00060.x

Kosobokova, K. N. (1999). The reproductive cycle and life history of the Arctic copepod *Calanus glacialis* in the White Sea. *Polar Biology, 22*(4), 254-263. doi:10.1007/s003000050418

Kwasniewski, S., Hop, H., Falk-Petersen, S., & Pedersen, G. (2003). Distribution of *Calanus* species in Kongsfjorden, a glacial fjord in Svalbard. *Journal of Plankton Research, 25*(1), 1-20. doi:10.1093/plankt/25.1.1

Leu, E., Søreide, J. E., Hessen, D. O., Falk-Petersen, S., & Berge, J. (2011). Consequences of changing sea-ice cover for primary and secondary producers in the European Arctic shelf seas: Timing, quantity, and quality. *Progress in Oceanography, 90*(1-4), 18-32. doi:10.1016/j.pocean.2011.02.004

Lischka, S., & Hagen, W. (2005). Life histories of the copepods *Pseudocalanus minutus, P. acuspes* (Calanoida) and *Oithona similis* (Cyclopoida) in the Arctic Kongsfjorden (Svalbard). *Polar Biology, 28*(12), 910-921. doi:10.1007/s00300-005-0017-1

Madsen, S. D., Nielsen, T. G., & Hansen, B. W. (2001). Annual population development and production by *Calanus finmarchicus, C.glacialis* and *C.hyperboreus* in Disko Bay, western Greenland. *Marine Biology, 139*(1), 75-93.

Mann, K. H., & Lazier, J. R. N. (2006). *Dynamics of marine ecosystems: Biological-Physical interactions in the oceans.* Pp: 264-269.UK: Blackwell Publishing.

Matlab R2016a (2016), Mathworks Inc., Natick, MA, USA.

Mundy, C. J., Barber, D. G., & Michel, C. (2005). Variability of snow and ice thermal, physical and optical properties pertinent to sea ice algae biomass during spring. *Journal of Marine Systems, 58*(3-4), 107-120. doi:10.1016/j.jmarsys.2005.07.003

Norkart AS (2017). Open Street Map, EEA CLC 2006. Retrevied May 14th 2017. URL: https//kart.1881.no.

Norwegian Ice Service – MET Norway, Norwegian Meteorological Institute (2017). Icecharts and ice information. Retrieved April 5th 2017. URL: http://polarview.met.no/index_HI.html.

Nielsen, T. G., Kjellerup, S., Smolina, I., Hoarau, G., & Lindeque, P. (2014). Live discrimination of *Calanus glacialis* and *C. finmarchicus* females: Can we trust phenological differences? *Marine Biology, 161*(6), 1299-1306. doi:10.1007/s00227-014-2419-5

Nilsen, F., Cottier, F., Skogseth, R., & Mattsson, S. (2008). Fjord-shelf exchanges controlled by ice and brine production: The interannual variation of Atlantic Water in Isfjorden, Svalbard. *Continental Shelf Research, 28*(14), 1838-1853. doi:10.1016/j.csr.2008.04.015

R Core Team (2016). R: A language and environment for statistical computing. R Foundation for Statistical Computing, Vienna, Austria. URL https://www.R-project.org/.

Rasband, W., 2011. ImageJ 1.50i. National Institutes of Health, USA. URL http://imagej.nih.gov/ij.

Renz, J., Peters, J., & Hirche, H. J. (2007). Life cycle of *Pseudocalanus acuspes* giesbrecht (Copepoda, Calanoida) in the central Baltic Sea: II. Reproduction, growth and secondary production. *Marine Biology, 151*(2), 515-527. doi:10.1007/s00227-006-0510-2

Runge, J. A., & Ingram, R. G. (1988). Underice grazing by planktonic, calanoid copepods in relation to a bloom of ice microalgae in southeastern Hudson-Bay. *Limnology and Oceanography, 33*(2), 280-286.

Saloranta, T. M., & Svendsen, H. (2001). Across the Arctic front west of Spitsbergen: high-resolution CTD sections from 1998-2000. *Polar Research, 20*(2), 177-184. doi:10.1111/j.1751-8369.2001.tb00054.x

Schlitzer, R., Ocean Data View, http://odv.awi.de, 2016.

Skardhamar, J., & Svendsen, H. (2010) Short-term hydrographic variability in a stratified Arctic fjord. *Vol. 344. Geological Society Special Publication* (pp. 51-60).

Søreide, J. E., Leu, E., Berge, J., Graeve, M., & Falk-Petersen, S. (2010). Timing of blooms, algal food quality and *Calanus glacialis* reproduction and growth in a changing Arctic. *Global Change Biology, 16*(11), 3154-3163. doi:10.1111/j.1365-2486.2010.02175.x

Støylen, E., & Fer, I. (2014). Tidally induced internal motion in an Arctic fjord. *Nonlinear Processes in Geophysics, 21*(1), 87-100. doi:10.5194/npg-21-87-2014

Stubner, E. I., Soreide, J. E., Reigstad, M., Marquardt, M., & Blachowiak-Samolyk, K. (2016). Year-round meroplankton dynamics in high-Arctic Svalbard. *Journal of Plankton Research, 38*(3), 522-536. doi:10.1093/plankt/fbv124

Svendsen, H., Beszczynska-Moller, A., Hagen, J. O., Lefauconnier, B., Tverberg, V., Gerland, S., . . . Dallmann, W. (2002). The physical environment of Kongsfjorden-Krossfjorden, an Arctic fjord system in Svalbard. *Polar Research, 21*(1), 133-166. doi:10.1111/j.1751-8369.2002.tb00072.x

Tande, K. S. (1991). *Calanus* in North Norwegian fjords and in the Barents Sea. *Polar Research, 10*(2), 389-407. doi:10.1111/j.1751-8369.1991.tb00661.x

UNESCO (1968). Zooplankton sampling; Monographs on oceanographic methodology. (http://unesdoc.unesco.org/images/0007/000715/071517eo.pdf).

Varpe, O. (2012). Fitness and phenology: annual routines and zooplankton adaptations to seasonal cycles. *Journal of Plankton Research, 34*(4), 267-276. doi:10.1093/plankt/fbr108

Vogedes, D., Varpe, O., Søreide, J. E., Graeve, M., Berge, J., & Falk-Petersen, S. (2010). Lipid sac area as a proxy for individual lipid content of Arctic calanoid copepods. *Journal of Plankton Research, 32*(10), 1471-1477. doi:10.1093/plankt/fbq068

Walkusz, W., Kwasniewski, S., Falk-Petersen, S., Hop, H., Tverberg, V., Wieczorek, P., & Weslawski, J. M. (2009). Seasonal and spatial changes in the zooplankton community of Kongsfjorden, Svalbard. *Polar Research, 28*(2), 254-281. doi:10.1111/j.1751-8369.2009.00107.x

Ward, P., & Hirst, A. G. (2007). Oithona similis in a high latitude ecosystem: abundance, distribution and temperature limitation of fecundity rates in a sac spawning copepod. *Marine Biology*, *151*(3), 1099-1110. doi:10.1007/s00227-006-0548-1

Weydmann, A., Søreide, J. E., Kwasniewski, S., Leu, E., Falk-Petersen, S., & Berge, J. (2013). Ice-related seasonality in zooplankton community composition in a high Arctic fjord. *Journal of Plankton Research, 35*(4), 831-842. doi:10.1093/plankt/fbt031

Willis, K., Cottier, F., Kwasniewski, S., Wold, A., & Falk-Petersen, S. (2006). The influence of advection on zooplankton community composition in an Arctic fjord (Kongsfjorden, Svalbard). *Journal of Marine Systems, 61*(1–2), 39-54. doi:http://dx.doi.org/10.1016/j.jmarsys.2005.11.013

Willis, K. J., Cottier, F. R., & Kwaśniewski, S. (2008). Impact of warm water advection on the winter zooplankton community in an Arctic fjord. *Polar Biology*, *31*(4), 475-481. doi:10.1007/s00300-007-0373-0

WoRMS Editorial Board (2017). World Register of Marine Species. Available from http://www.marinespecies.org at VLIZ.

Appendix A

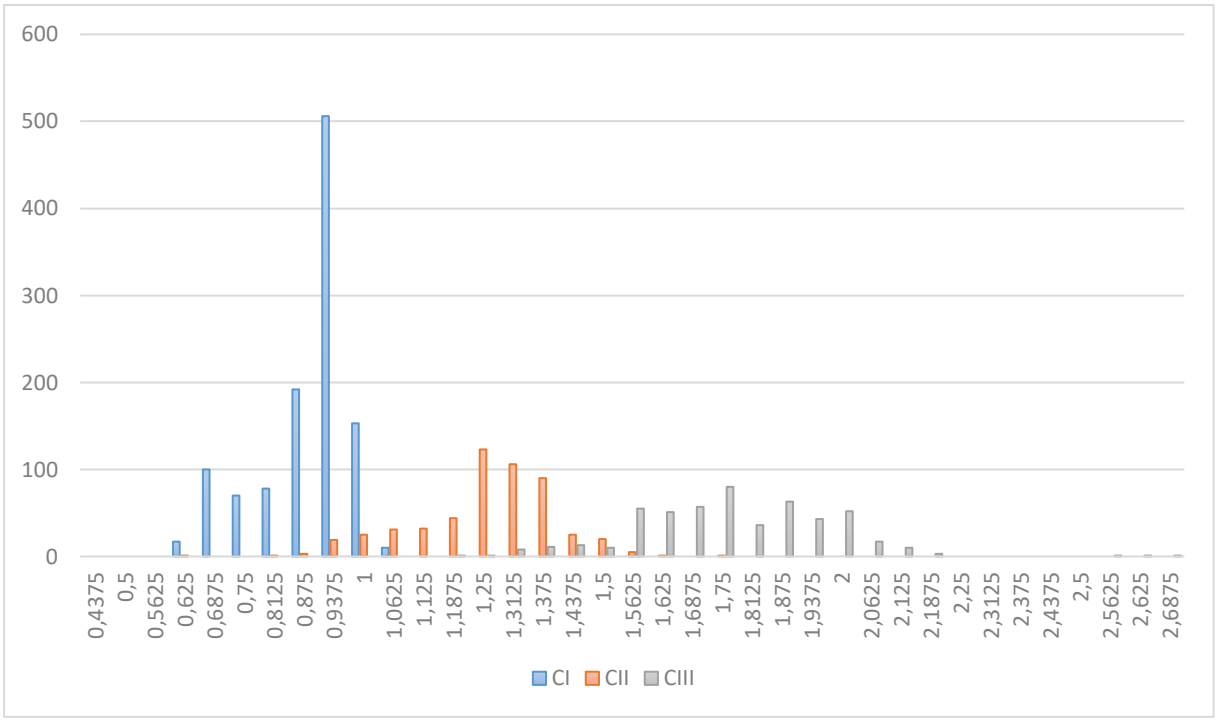

Figure A.15 *Calanus* spp length distribution for stages CI-CIII in mm

Appendix B

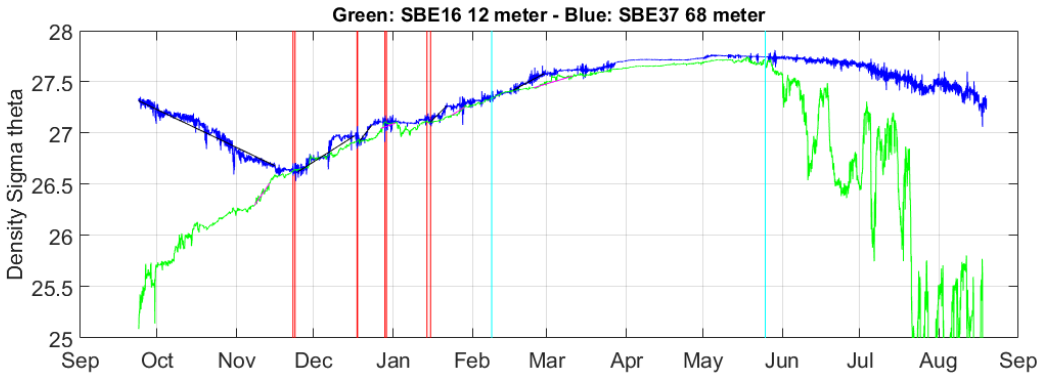

Figure B.16 Density time series from the mooring site in the inner part of the fjord at depths 12 m - Green and 68 m - Blue

Appendix C

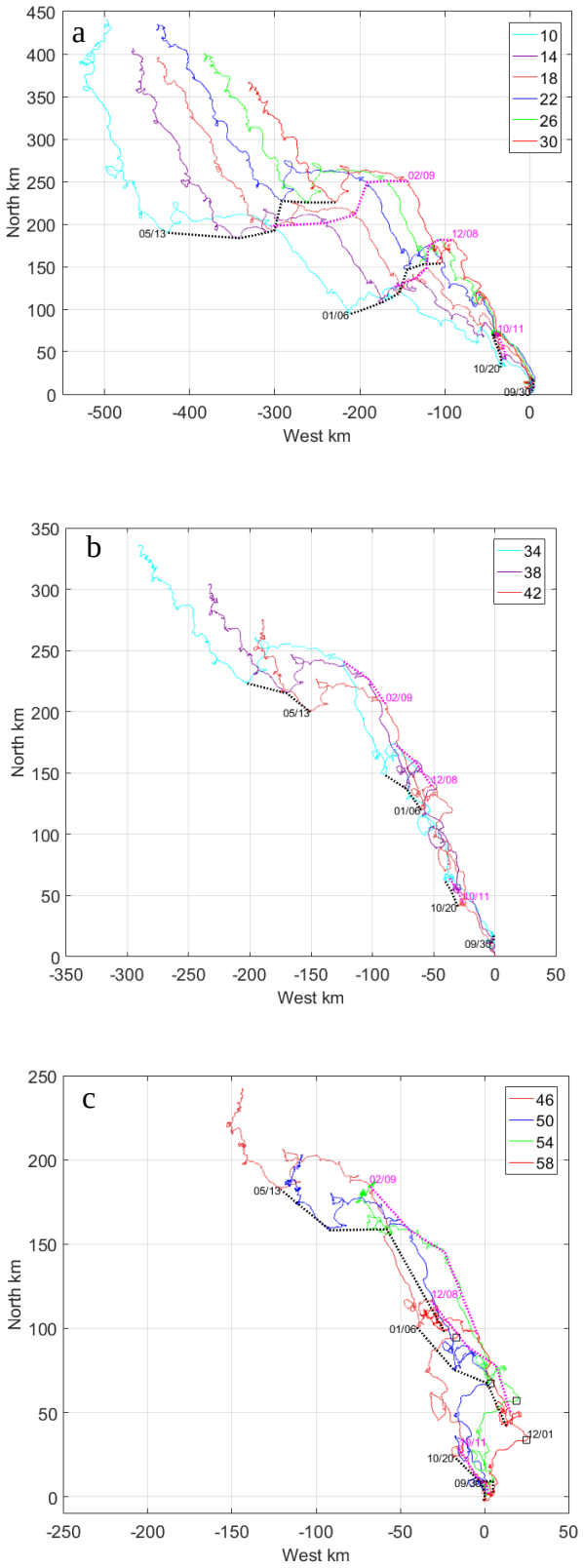

Figure C.17a b c Progressive vector diagrams indicating the prevailing current directions at the mooring site at different depths

Appendix D

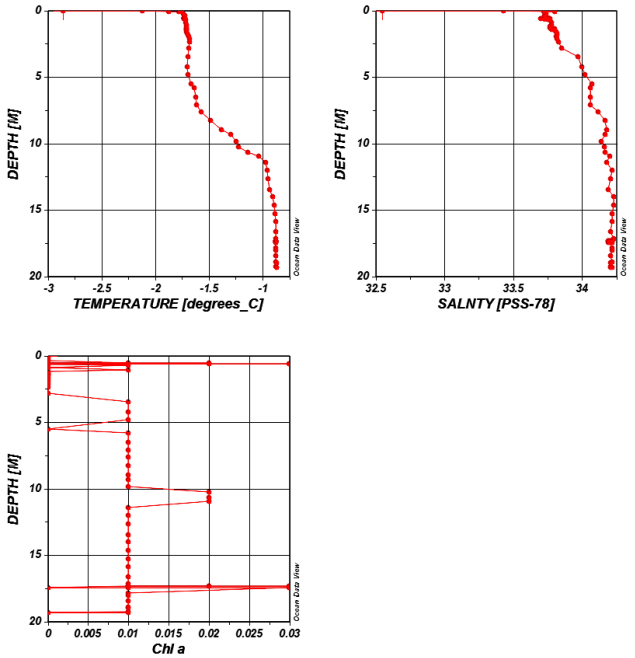

Figure D.18 CTD profile from vMF X

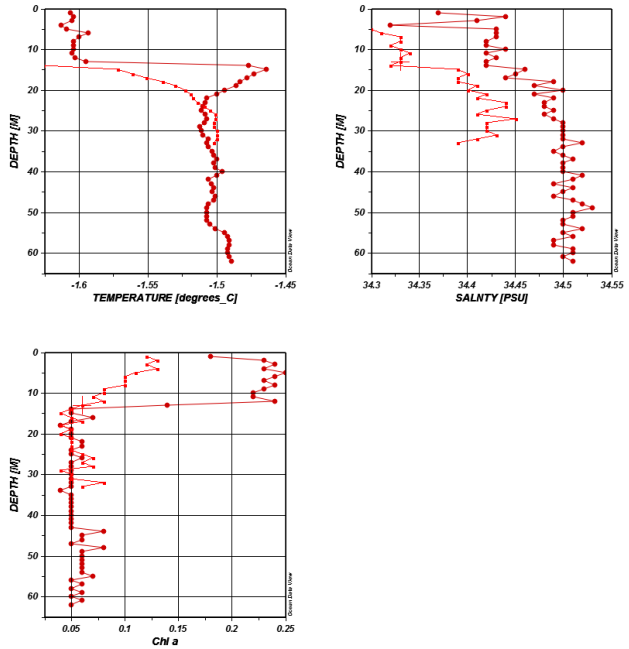

Figure D.19 CTD profile from vMF Y. Two profiles were taken at this station, with some distance between. The zooplankton samples are taken at the shallowest site (light red), while only the CTD profile was taken at the deep site (dark red)

Appendix E

Table E.7 Integrated Chl-*a* values in mg m^{-2}

	April 30th – May 1st	June 3rd – June 4h (mg m^{-2})	July 2nd – July 4th
vMF 1		65.66	0.98
vMF 4	79.48		
vMF 5		72.97	
vMF 9	441.44	70.56	

Appendix F

Table F.8 Species list over all species and their abundance at vMF 1 every month. vMF 1 was not reached in March and April, therefore abundance from vMF X and vMF Y is shown. Abundance is based on the whole water column and calculated as an average from three replicates in ind. m^{-3} ± standard deviation. *Chaetognatha juveniles, not able to determine to species.

	Sept. 2015	**Mar. 2016 vMF X**	**April 2016 vMF Y**	**15th May 2016**	**June 2016**	**July 2016**	**Aug. 2016**
PHYLUM ANNELIDA							
CLASS POLYCHAETA							
Polychaeta larvae	-	261.5±156.3	18.4±17.7	43.7±14.3	552.0±75.6	34.7±31.1	5.0±8.8
PHYLUM ARTHROPODA							
CLASS HEXANAUPLIA							
Cirripedia nauplii	-	-	-	595.0±234.1	12852.1±4236.9	2.8±4.8	-
ORDER CALANOIDA							
Acartia longiremis	2.0±3.5	-	0.6±1.1	8.0±3.7	13.5±10.4	11.7±10.4	63.4±46.6
Bradyidius similis	-	-	-	-	-	-	0.1±0.1
Calanus finmarchicus	405.3±76.7	12.0±5.3	6.2±2.1	4.1±1.0	27.9±13.6	150.7±51.2	629.4±174.4
Calanus glacialis	2055.1±344.0	48.6±31.8	44.0±22.1	38.6±8.7	1441.2±594.2	555.7±67.5	1204.5±.484.9
Calanus hyperboreus	-	1.2±2.1	-	2.0±2.1	1.5±0.1	2.1±2.0	11.4±9.8
Gaetanus spp.	-	-	-	1.4±1.2	-	-	0.0±0.1
Metridia longa	-	-	0.3±0.6	2.1±2.1	-	5.5±6.1	8.6±14.8
Microcalanus spp.	-	13.2±9.4	87.3±40.9	187.4±54.6	95.0±12.1	31.6±14.6	12.8±13.6
Pseudocalanus spp.	1636.6±384.3	333.6±184.2	144.4±75.2	194.8±11.4	310.0±91.2	822.52±254.7	1725.6±180.0
ORDER CYCLOPOIDA							
Oithona atlantica	-	-	-	2.7±3.2	38.0±14.2	10.8±13.4	21.9±33.1
Oithona similis	694.9±348.4	84.5±43.4	67.0±36.7	98.48±3.0	213.0±85.7	359.4±38.9	4405.9±1313.6
ORDER HARPACTICOIDA							
Harpacticoida spp.	-	-	-	1.4±2.4	12.8±11.3	1.3±2.3	-
Microsetella norvegica	-	40.5±37.5	36.8±13.8	-	6.7±11.6	3.7±4.6	40.9±24.9

	Sept. 2015	Mar. 2016 vMF X	April 2016 vMF Y	15th May 2016	June 2016	July 2016	Aug. 2016
ORDER POECILOSTOMATOIDA							
Triconia borealis	12.2±10.6	31.9±14.4	65.1±22.9	13.9±6.5	11.43±6.0	17.8±11.59	63.7±8.7
CLASS MALACOSTRACA							
ORDER AMPHIPODA							
Apherusa glacilis	0.0±0.0	-	-	-	-	-	-
Themisto abyssorum	0.5±0.3	-	-	0.1±0.1	1.0±0.2	0.5±0.1	0.1±0.1
Themista libellula	0.0±0.0	-	-	-	-	-	-
ORDER DECAPODA							
Pagurus pubescense	-	-	-	-	-	-	0.0±0.1
Zoea	-	-	-	1.3±1.2	211.6±182.7	0.3±0.1	2.0±3.4
ORDER EUPHAUSIACEA							
Euphausiid nauplii	-	-	-	2.5±4.4	86.7±23.1	0.1±0.1	-
Furcilia	-	-	-	0.1±0.0	0.5±0.4	0.1±0.1	-
Thysanoessa inermis	0.2±0.2	-	-	-	-	-	-
Thysanoessa rachii	-	-	-	-	-	-	-
CLASS OSTRACODA							
Ostracoda spp.	-	1.3±2.3	-	0.7±1.2	29.5±12.3	551.0±39.2	6.7±5.8
PHYLUM BRYOZOA							
Bryozoa larvae	-	9.1±6.1	7.3±3.9	-	1.5±1.6	0.7±1.3	43.7±31.4
PHYLUM CHAETOGNATHA	-	0.3±0.5*	0.9±0.8*	0.4±0.6*	-	-	-
CLASS SAGITTOIDEA							
ORDER APHRAGMOPHORA							
Parasagitta elegans	20.0±1.1	1.2±0.6	1.0±0.8	1.9±0.8	21.8±11.1	6.5±2.6	17.5±1.4
ORDER PHRAGMOPHORA							

	Sept. 2015	Mar. 2016 vMF X	April 2016 vMF Y	15th May 2016	June 2016	July 2016	Aug. 2016
Eukrohnia hamata	-	0.2±0.3	-	0.5±0.2	1.0±0.4	0,1±0,1	-
PHYLUM CHORDATA							
CLASS APPENDICULARIA							
ORDER COPELATA							
Appendicularia spp.	105.7±39.7	-	-	-	-	-	93.0±42.0
PHYLUM CNIDARIA							
CLASS ANTHOZOA							
Anthozoa juvenile	4.1±7.0	1.5±1.8	2.5±2.9	2.0±0.1	6.5±9.0	1.3±2.3	7.5±3.4
CLASS HYDROZOA	-	-	-	0.1±0.0	0.9±0.2	0.2±0.1	0.1±0.1
PHYLUM CTENOPHORA	0.6±0.1	-	0.1±0.1	0.5±0.2	-	0.1±0.1	0.2±0.2
PHYLUM ECHINODERMATA							
Echinodermata larvae	-	-	-	-	5.6±9.6	2.2±3.9	58.6±22.3
PHYLUM MOLLUSCA							
CLASS BIVALVIA							
Bivalve veligers	6.1±6.1	-	-	2.7±1	6.6±8.9	14037.7±1290.2	6512.1±3379.2
CLASS GASTROPODA							
ORDER GYMNOSOMATA							
Clione limacina	-	-	-	-	0.1±0.1	-	0.0±0.1
ORDER THECOSOMATA							
Limacina juvenile	8.1±9.3	6.8±6.5	2.5±2.9	-	-	-	-
Limacina helicina	-	-	-	0.1±0.1	0.1±0.1	1.1±0.7	495.7±153.2
Limacina retroversa	-	-	-	-	0.1±0.2	-	4.8±4.9

Table F.9 Species list over all species and their abundance at vMF 5 every month. Sampling in April was conducted at vMF 4 due to high fluorescence readings. Abundance is based on the whole water column and calculated as an average from three replicates in ind. m^{-3} ± standard deviation. *Chaetognatha juveniles, not able to determine to species.

	Sept. 2015	**30th April 2016 vMF 4**	**June 2016**	**July 2016**	**Aug. 2016**
PHYLUM ANNELIDA					
CLASS POLYCHAETA					
Polychaeta larvae	-	165.0±95.2	534.2±134.6	69.1±4.3	6.2±5.4
PHYLUM ARTHROPODA					
CLASS HEXANAUPLIA					
Cirripedia nauplii	-	2440.2±940.7	4861.0±1391.9	65.8±11.1	-
ORDER CALANOIDA					
Acartia longiremis	42.7±16.0	9.7±11.1	8.5±7.6	132.5±70.6	76.0±55.2
Bradyidius similis	-	-	-	-	-
Calanus finmarchicus	126.4±13.8	28.5±20.0	124.3±53.9	1371.2±201.3	1581.1±1259.1
Calanus glacialis	147.2±1.2	64.4±33.7	1647.8±494.1	2307.0±777.0	1231.6±116.0
Calanus hyperboreus	3.3±2.9	0.1±0.2	9.8±6.1	0.8±1.4	4.4±7.7
Gaetanus spp.	1.8±3.1	-	3.7±6.4	3.3±2.9	3.1±5.4
Metridia longa	-	2.6±3.6	6.4±4.2	1.7±2.9	6.2±10.7
Microcalanus spp.	8.9±11.1	100.0±83.8	46.9±9.6	11.5±5.7	29.9±18.4
Pseudocalanus spp.	567.1±21.6	120.4±33.6	126.6±22.6	1143.2±78.9	3206.5±870.8
ORDER CYCLOPOIDA					
Oithona atlantica	8.9±11.1	-	1.5±1.8	-	8.9±15.4
Oithona similis	1086.2±138.7	157.2±21.0	109.4±24.0	1780.3±102.7	14578.2±10265.9
ORDER HARPACTICOIDA					
Harpacticoida spp.	-	1.6±1.4	7.4±6.4	9.9±17.1	-
Microsetella norvegica	-	12.3±8.6	14.8±25.7	7.4±12.8	80.0±58.3
ORDER POECILOSTOMATOIDA					
Triconia borealis	1.8±3.1	28.9±10.9	0.6±1.1	20.6±6.2	70.4±13.4
CLASS MALACOSTRACA					
ORDER AMPHIPODA					
Apherusa glacilis	-	-	-	-	-

	Sept. 2015	30th April 2016 vMF 4	June 2016	July 2016	Aug. 2016
Themisto abyssorum	0.1±0.1	0.1±0.1	3.0±2.4	1.0±0.1	0.2±0.2
Themista libellula	-	-	-	-	-
ORDER DECAPODA					
Pagurus pubescense	0.0±0.0	-	-	-	-
Zoea	-	1.5±1.0	7.3±3.8	3.2±2.0	0.2±0.1
ORDER EUPHAUSIACEA					
Euphausiid nauplii	-	3.8±4.7	140.8±17.0	14.8±25.8±25.7	-
Furcilia	-	0.1±0.1	0.2±0.2	0.2±0.2	0.2±0.0
Thysanoessa inermis	0.0±0.0	-	-	-	-
Thysanoessa rachii	-	-	-	0.0±0.0	-
CLASS OSTRACODA					
Ostracoda spp.	-	-	69.3±32.8	2842.8±437.9	-
PHYLUM BRYOZOA					
Bryozoa larvae	5.3±5.3	-	-	-	57.3±33.7
PHYLUM CHAETOGNATHA	-	1.2±1.1*	0.1±0.2*	7.7±12.9*	-
CLASS SAGITTOIDEA					
ORDER APHRAGMOPHORA					
Parasagitta elegans	2.9±0.4	8.1±0.9	25.1±10.9	190.2±304.0	16.4±3.8
ORDER PHRAGMOPHORA					
Eukrohnia hamata	-	0.7±0.5	0.5±0.4	7.6±12.9	0.1±0.1
PHYLUM CHORDATA					
CLASS APPENDICULARIA					
ORDER COPELATA					
Appendicularia spp.	56.9±43.4	-	0.2±0.3	1.7±2.9	399.3±148.2
PHYLUM CNIDARIA					
CLASS ANTHOZOA					
Anthozoa juvenile	-	45.9±39.9	-	-	-
CLASS HYDROZOA	0.0±0.0	0.3±0.3	1.4±0.9	0.4±0.4	0.1±0.1

	Sept. 2015	30th April 2016 vMF 4	June 2016	July 2016	Aug. 2016
PHYLUM CTENOPHORA	0.5±0.2	1.1±1.0	0.1±0.2	0.4±0.4	0.1±0.1
PHYLUM ECHINODERMATA					
Echinodermata larvae	19.6±3.1	5.7±3.7	1.8±2.4	161.3±111.1	12.0±13.5
PHYLUM MOLLUSCA					
CLASS BIVALVIA					
Bivalve veligers	1.8±3.1	2.8±4.8	-	30484.8±3180.7	8287.3±6164.7
CLASS GASTROPODA					
ORDER GYMNOSOMATA					
Clione limacina	-	-	-	0.0±0.1	-
ORDER THECOSOMATA					
Limacina juvenile	-	4.9±2.4	-	160.5±15.4	275.4±202.2
Limacina helicina	17.8±22.2	0.3±0.1	0.1±0.1	0.7±0.5	1139.2±373.3
Limacina retroversa	-	-	-	0.0±0.1	-